Journal of Medicinal Chemistry

Article

Design, Synthesis, and Pharmacological Evaluation of Second-Generation Tetrahydroisoquinoline-Based CXCR4 Antagonists with Favorable ADME Properties

Huy H. Nguyen, Michelle Bora Kim, Robert J Wilson, Christopher Butch, Katie M Kuo, Eric J Miller, Yesim A Tahirovic, Edgars Jecs, Valarie M Truax, Tao Wang, Chi Sum, Mary Ellen Cvijic, Gretchen M Schroeder, Lawrence J Wilson, and Dennis C. Liotta

J. Med. Chem., **Just Accepted Manuscript** • DOI: 10.1021/acs.jmedchem.8b00450 • Publication Date (Web): 27 Jul 2018

Just Accepted

ACS Publications

is published by the American Chemical Society. 1155 Sixteenth Street N.W., Washington, DC 20036

Design, Synthesis, and Pharmacological Evaluation of Second-Generation Tetrahydroisoquinoline-Based CXCR4 Antagonists with Favorable ADME Properties

Huy H. Nguyen,[†] Michelle B. Kim,[†] Robert J. Wilson,[†] Christopher J. Butch,[†] Katie M. Kuo,[†] Eric J. Miller,[†] Yesim A. Tahirovic,[†] Edgars Jecs,[†] Valarie M. Truax,[†] Tao Wang,[‡] Chi S. Sum,[‡] Mary E. Cvijic,[‡] Gretchen M. Schroeder,[‡] Lawrence J. Wilson,[†*] and Dennis C. Liotta[†*]

[†]Department of Chemistry, Emory University, 1515 Dickey Drive NE, Atlanta, Georgia 30322, United States

[‡]Bristol-Myers Squibb Research & Development, Route 206 and Province Line Road, Princeton, New Jersey 08543, United States

KEYWORDS

G-protein coupled receptor, CXCR4 receptor, SDF-1, calcium flux, CXCR4 antagonists, immuno-oncology, piperazine, tetrahydroquinoline, tetrahydroisoquinoline, Muscarinic receptor, liver microsomes, permeability, CYP450

ABSTRACT

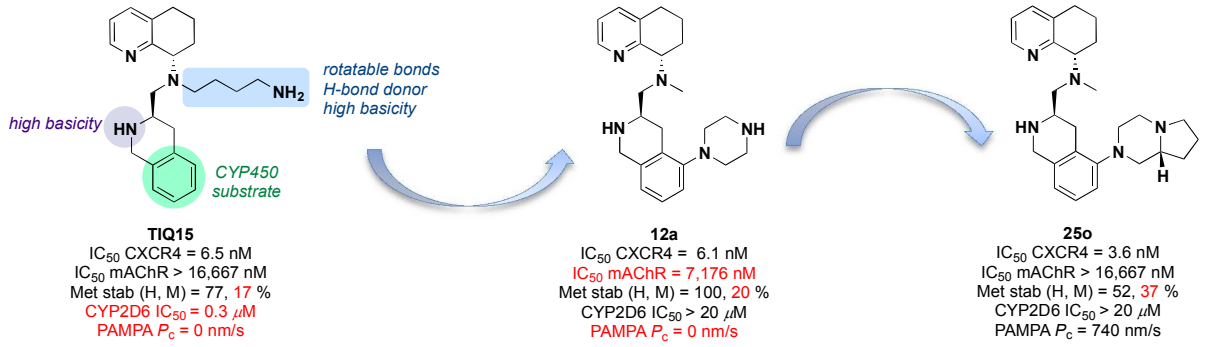

Abstract Figure

CXCR4 is a G protein-coupled receptor that interacts with its cognate ligand CXCL12 to synchronize many physiological responses and pathological processes. Disruption of the CXCL12-CXCR4 circuitry by small molecule antagonists has emerged as a promising strategy for cancer intervention. We previously disclosed a hit-to-lead effort that led to the discovery of a series of tetrahydroisoquinoline-based CXCR4 antagonists exemplified by the lead compound TIQ15. Herein, we describe our medicinal chemistry efforts toward the redesign of TIQ15 as a result of high mouse microsomal clearance, potent CYP2D6 inhibition, and poor membrane permeability. Guided by the *in vitro* ADME data of TIQ15, structural modifications were executed to provide compound **12a** which demonstrated a reduced potential for first-pass metabolism while maintaining the CXCR4 potency. Subsequent SAR studies and multiparameter optimization of **12a** resulted in the identification of compound **25o**, a highly potent, selective, and metabolically stable CXCR4 antagonist possessing good intestinal permeability and low risk of CYP-mediated drug-drug interactions.

INTRODUCTION

The C-X-C chemokine receptor type 4 (CXCR4) is a member of the heptahelical G-protein coupled receptor (GPCR) superfamily and broadly expressed on the surface of many important cell types, including, but not limited to, hematopoietic stem cells,[1] leukocytes,[2] endothelial cells,[3] and tumor cells.[4] Activation of CXCR4 through its binding of endogenous chemokine ligand CXCL12[5] (SDF-1, stromal cell-derived factor-1) triggers downstream signaling cascades that result in a breadth of biological processes.[6] Beyond its historically-known function as a co-receptor harnessed by T-tropic (X4) HIV strains for entry into $CD4^+$ T cells,[7] CXCR4 has been implicated in the pathogenesis of cancer.[8]

Over the past decade, the CXCR4/CXCL12 axis has garnered considerable attention from the scientific community due to its complex involvements in a wide range of oncogenic processes.[9] Several recent reports have demonstrated the aberrantly high expression of CXCR4 in more than 23 types of human malignancies where tumor cells exploit CXCR4-mediated chemotactic signaling to evade immune surveillance.[10] In this regard, the intratumoral secretion of CXCL12 stimulates pro-survival signaling within the tumor microenvironment and recruits $CXCR4^+$ immunosuppressive leukocytes to subvert T cell–mediated antitumor immune responses. CXCL12 also plays a major role in recruiting $CXCR4^+$ pro-angiogenic cells which support revascularization of ischemic tissue and tumor growth.[11] $CXCR4^+$ cancer cells take advantage of the CXCL12 chemoattractant gradient to migrate to distant tissues, which defines the phenomenon known as metastasis.[12] Blockade of CXCL12-mediated CXCR4 activity by small molecule inhibitors has been shown to effectively reverse tumor-influenced immunosuppression in preclinical models recapitulating human metastatic breast, ovarian, and pancreatic cancer.[13] These studies demonstrated that AMD3100 (**1**, Figure 1), a small molecule CXCR4 antagonist, selectively reduced intratumoral infiltration of $FoxP3^+$ regulatory T cells and

alternatively induced rapid $CD8^+$ effector T cell accumulation in the tumor microenvironment, resulting in increased tumor cell apoptosis and necrosis, reduced intraperitoneal dissemination, and improved overall survival. As such, CXCR4 represents an attractive therapeutic target for the development of novel anticancer drugs.

To date, a diverse array of CXCR4 antagonists, both peptides and small molecules, have been disclosed in the literature as recently reviewed elsewhere.[14] First-generation antagonists comprise bicyclam AMD3100 and simplified analogues thereof.[15] This compound initially entered clinical trials as an anti-HIV agent but later emerged on the market as an FDA-approved stem cell mobilizer (AMD3100, **1**, Figure 1) following a serendipitous discovery in the clinic.[16] In addition to its clinical utility, AMD3100 has been extensively employed as a "proof-of-concept" tool molecule to elucidate the role of CXCR4 in a variety of preclinical cancer models.[17] Accordingly, numerous academic research groups and pharmaceutical companies have devoted significant efforts into the search of next generations of CXCR4 antagonists combining high potency with acceptable oral bioavailability. These efforts resulted in a plethora of chemotypes including the first orally active agent AMD11070 (**2**), which is currently in phase 2 clinical trials for WHIM syndrome.[18] The discovery of AMD11070 laid the foundation for the development of more advanced preclinical leads. For instance, an extensive optimization campaign of AMD11070 at GlaxoSmithKline produced GSK812397 (**3**).[19] Researchers at Norvatis also identified IT1t (**4**) via high-throughput screening and optimization of an isothiourea series.[20]

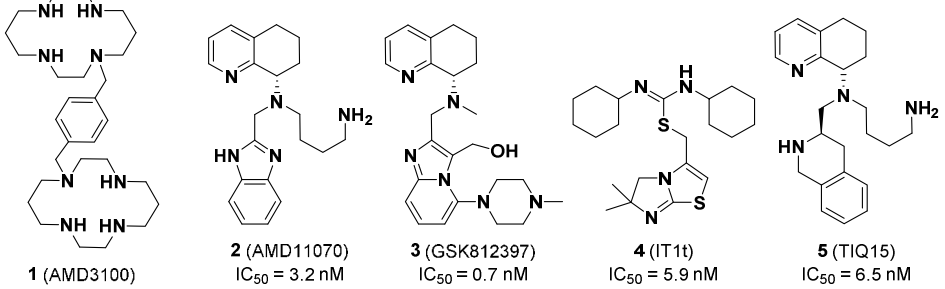

Figure 1. Literature Small-Molecule CXCR4 Antagonists.

Our own efforts in this area have yielded three attractive chemotypes.[21] Most prominent is the tetrahydroisoquinoline(THIQ)-based series, exemplified by lead compound TIQ15 (**5**), a highly potent and selective antagonist. However, upon a thorough assessment of drug-like properties, we found TIQ15 suffered from intermediate clearance in mouse hepatic microsomes (17% remaining after 10 minutes) and poor predicted intestinal permeability (P_c = 0 at pH 7.4) by the PAMPA assay result, both of which hamper further *in vivo* efficacy studies in murine models. More importantly, TIQ15 inhibits cytochrome P450 (CYP) 2D6 isozyme at submicromolar concentrations (IC_{50} = 0.3 μM) which is indicative of high propensity for drug-drug interactions that could restrict its use in combination therapy regimens. Together, these shortcomings prompted our medicinal chemistry efforts toward redesigning the TIQ15 chemotype to attain a better alignment of ADME attributes. Herein, we describe the structure-based design, efficient parallel synthesis, and pharmacological evaluation of a novel series of CXCR4 antagonists that culminated in the discovery of highly potent lead compound **25o** exhibiting favorable *in vitro* pharmacokinetics properties.

RESULTS AND DISCUSSION

Redesign Criteria. To determine suitable chemical modifications, we carefully examined structural features of TIQ15 to identify regions on the molecule that account for pharmacokinetic

liabilities. Particularly notable is the butyl amine moiety which has 5 rotatable bonds, 2 hydrogen bond donors (HBD), and high basicity (estimated pK_a = 10.7). Indeed, the poor passive permeability of TIQ15 is attributed to the high basicity arising from the butyl amine and the THIQ heterocycle (estimated pK_a = 9.6). Our NMR studies showed both of these amine centers were protonated at physiological pH (data not shown), thus likely impeding the diffusion of the molecule across lipid-coated membranes. In addition, metabolite identification studies on TIQ15, after incubation with mouse hepatocytes, revealed the formation of two oxidative metabolites (M + 16) of the (*S*)-tetrahydroquinoline (THQ) moiety. By leveraging the outcomes of these studies, we successfully removed metabolic liability through modifications of THQ core.[22] However, we further postulated that the first-pass metabolism could be ascribed to CYP-mediated oxidation at the benzylic and aromatic positions of the THIQ ring. As a result, this optimization campaign focused on three key objectives. The first was to reduce the number of rotatable bonds which has been demonstrated to improve pharmacokinetic and pharmacological profiles based on the retrospective analysis of a large collection of pharma compounds.[23] Second, we sought to suppress CYP-mediated oxidative metabolism to the THIQ ring and attenuate CYP inhibition by introducing substituents to stereo-electronically block CYP enzymes from accessing metabolic soft spots. Finally, we aimed to enhance the intestinal permeability by increasing the lipophilicity as well as reducing HBD counts and basicity of amine centers.

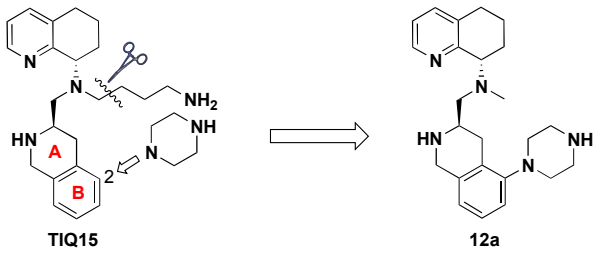

Figure 2. ADME improvement-based redesign strategy.

Taking these criteria into account, we decided to truncate the butyl amine side chain on the central nitrogen and conformationally constrain the distal amine moiety by incorporating it into a piperazine ring directly attached to the THIQ core (Figure 2). We chose the piperazine motif as a surrogate for the butyl amine since this ubiquitous pharmacophore is present in numerous GPCR ligands,[24] including CCR5,[25] CXCR3,[26] and CXCR4 antagonists.[19a-c, 19e] To attach the piperazine on the THIQ, we looked for synthetically tractable and operationally straightforward transformations amenable to rapid SAR exploration. We envisioned that chemically modifying the benzylic position of the A-ring would be challenging and generate an additional chiral center. Conversely, decorating the aromatic B-ring with the piperazine would be more accessible through well-documented transformations, *e.g.*, Buchwald-Hartwig amination or nucleophilic aromatic substitution (S_NAr), and thus was pursued in this medicinal chemistry program. We hypothesized that appending the piperazine at the C-2 position would achieve a twofold objective: (1) hinder the exposure of this portion of the molecule to CYP enzymes and (2) orchestrate the distal piperazine nitrogen to gyrate a similar spatial trajectory as the butyl amine nitrogen. To validate the latter, a molecular mechanics based analysis of the conformational overlay of the two scaffolds was conducted with the goal of understanding the spatial coincidence of the distal nitrogen pharmacophore relative to the common structural backbone. This analysis considered all conformers of both molecules with a relative energy of less than 3 kcal·mol^{-1} relative to the global minimum and with a 0.1Å RMSD resolution. All conformers were then positioned based on a minimum RMSD alignment of the maximally common heavy atom substructure, and the positions of the distal nitrogen were plotted in 3D space, as depicted in Figure 3. This depiction exhibited that approximately 10% of the

conformers for each scaffold existed inside a toroidal overlapping region centered between the THQ and THIQ rings. Further, many of these conformers were of low energy relative to the global minima, demonstrating that occupancy of this toroidal region will be high for each scaffold. Finally, adjacent low energy structures were found to exhibit good alignment of the common backbone (see Figure 3), which further supports the hypothesized conformational similarity of the pharmacophore positioning between the two scaffolds. This crude analysis provided reasonable anticipation that compound **12a** embodying a piperazinyl tetrahydroisoquinoline motif would offer similar potency and hence gave us reason to investigate this new series.

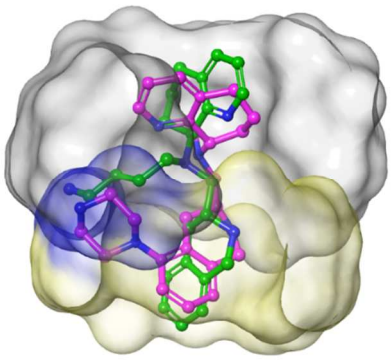

Figure 3. Conformational overlay of **12a** (magenta) and TIQ15 (green). A 3D-pharmacophore model was generated by *in silico* conformational analysis of TIQ15 and the target compound **12a** wherein low energy conformers of these compounds were generated and superimposed. The gray and yellow clouds represent the possible positions of the distal nitrogen pharmacophore of TIQ-15 and **12a**, respectively, relative to the common backbone. The areas of overlap at the figure center (indicated by the blue cloud) are representative of the pool of conformers (~10% of the total for each species) which can adopt similar positioning of the ring and nitrogen pharmacophores. The depicted structures are conformational minima identified within the regions of overlap. Graphics were generated with Maestro v9.7.

Preliminary Synthesis and Screening. Since the THQ and THIQ motifs were kept intact, the new molecular scaffold contained the same stereogenic centers as TIQ15. Though in TIQ15 series we demonstrated the *anti*-diastereomer with the (*R*) configuration at the THIQ ring chiral center was 80-fold more potent than the other isomeric counterpart, we were uncertain if similar

stereochemical preference would translate to the new series. For that reason, the initial synthesis of compound **12a** was deliberately achiral so that both diastereomers could be prepared and tested to determine the optimal stereochemistry for the activity. As depicted in Scheme 1, the route commenced with the *N*-Boc protection of commercially available racemic THIQ building block **6** to provide ester **7**. Coupling of **7** with 1-Boc-piperazine under typical Buchwald-Hartwig amination conditions proceeded smoothly to afford ester **8**. DIBAL-H reduction of ester **8** to aldehyde **9** followed by $NaBH(OAc)_3$ mediated reductive amination with (*S*)-*N*-methyl-5,6,7,8-tetrahydroquinolin-8-amine **10** furnished two diastereomers **11a** and **11b** which were readily separated by column chromatography. Global deprotection of Boc groups with TFA delivered final compounds as free amines **12a** (*S,R*) and **12b** (*S,S*). Since CXCR4 activation initiates G protein-mediated intracellular Ca^{2+} release, the antagonism of CXCR4 was measured using CXCL12-induced Ca^{2+} flux inhibition assay. The screening revealed a 50-fold difference in activity with **12a** being the more potent isomer, IC_{50} of 6.1 nM versus 313.8 nM (**12b**). It was noteworthy that **12a** fully retained the potency of the parent compound TIQ15, suggesting validity to the pharmacophore model (*vide supra*).

Scheme 1. Preparation of 12a, 12b and 30[α]

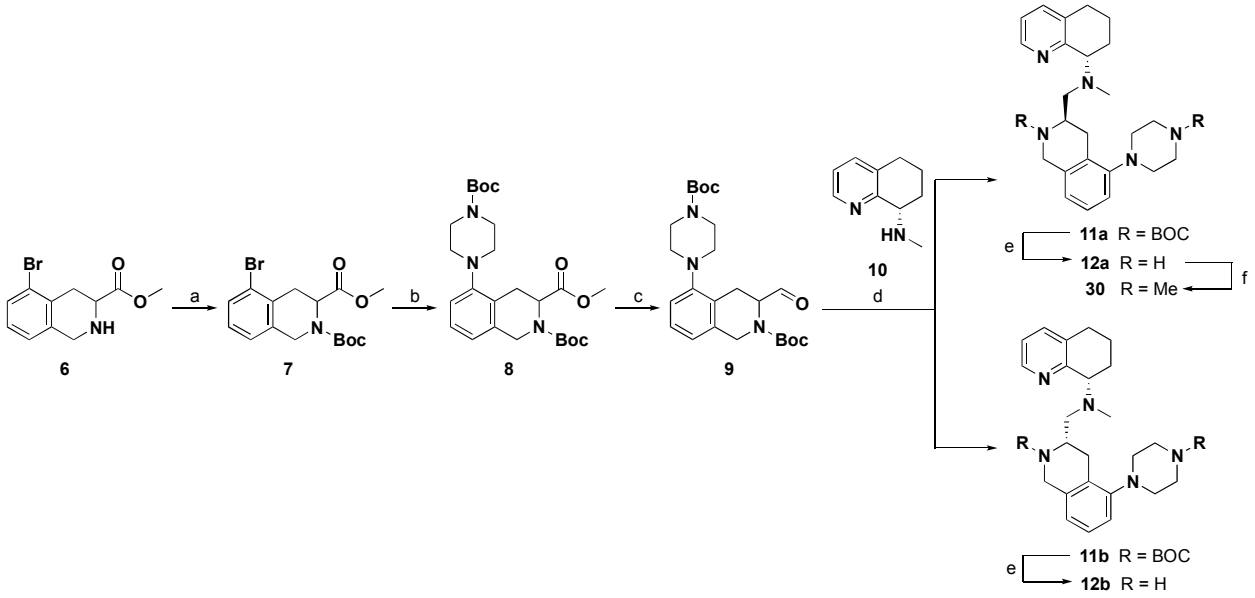

[a]Reagents and conditions: (a) Boc_2O, $NaHCO_3$, 1,4-dioxane, rt; (b) 1-Boc-piperazine, $Pd_2(dba)_3$, (±)-BINAP, Cs_2CO_3, toluene, 120 ºC, sealed tube; (c) DIBAL-H, toluene, -78 ºC; (d) **10**, $NaBH(OAc)_3$, 1,2-DCE, rt; (e) TFA, DCM, rt; (f) paraformaldehyde, $NaBH(OAc)_3$, 1,2-DCE, rt.

Table 1. Comparative In Vitro Profiling of TIQ15, 12a, and 12b

Compd	CXCR4 Ca^{2+} Flux IC_{50} (nM)[a,g]	mAChR Ca^{2+} Flux IC_{50} (μM)[h]	Microsomal Stability % remaining[b,h]		Inhibition of CYP450 2D6 IC_{50} (μM)[c,h]	hERG binding IC_{50} (μM)[d,h]	PAMPA permeability P_c (nm/s)[e,g]
			Human	Mouse			
TIQ15	6.25±2.05	>33.3	77.0	17.0	0.320	8.92	0
12a	6.08±1.43	7.18	99.7	19.9	>20.0	20.3	0
12b	313±93.1	2.10	94.2	54.6	>20.0	ND[f]	4.00±6.00

[a]Concentration of compound inhibiting the CXCR4 Ca^{2+} flux/release by 50%. [b]Metabolism by microsomes (CYP450 and other NADP-dependent enzymes) was monitored and expressed at % remaining after 10 minutes. [c]The lower limit (< 20 μM) in the CYP450 assays (3A4, 2D6) is shown; all compounds >20 μM against 3A4. [d]Binding displacement of [^{3}H]astemizole in HEK membranes that overexpress hKv11.1. [e]Measured at pH 7.4. [f]ND = not determined. [g]n=2, reported error represents standard deviation. [h]n=1.

Next, to establish the benchmark data for the new series, compound **12a** was extensively profiled in a series of pharmacological assays designed to predict aspects of pharmacokinetic and pharmacodynamic performance (Table 1). We were gratified to find significant improvements in the profiles of **12a**. Compound **12a** is unlikely to be a perpetrator of drug-drug interactions based on the lack of inhibitory activity towards the most notable human CYP450 enzymes 3A4 and 2D6. Unfortunately, the permeability issue still lingered (P_c = 0 at pH 7.4). Compound **12a** was predicted to have low potential for QT interval prolongation and cardio toxicity on the basis of a

weak human ether-à-go-go-related gene (*h*ERG) binding signal (IC_{50} = 20.3 μM) and the absence of antagonist activity in L-type Ca^{2+} channel assay (IC_{50} > 80 μM). However, upon an assessment of potential off-target activities, compound **12a** displayed a weak inhibition against mixed M_1, M_3, M_5 subtypes of muscarinic acetylcholine receptors (mAChR) (IC_{50} of 7.2 μM). Since these mAChRs play fundamental roles in many bodily functions,[27] it is essential to minimize or eliminate this off-target activity during early discovery phase to avoid cholinergic side effects, cardiovascular, and gastrointestinal adverse events as the compound progresses toward clinical trials. Taken together, compound **12a** represented a viable series with potentially divergent SAR.

Structure−Activity Relationship (SAR) Studies. The truncation of the butyl amine opened up a number of possibilities for side chain attachments on the central nitrogen, thus offering a productive avenue for SAR. The route delineated in Scheme 1 was adapted for the synthesis of side-chain modified analogues of **12a**. Having determined that the *R*-isomer **12a** was more potent than the *S*-isomer **12b**, we embarked on a synthetic route that tapped into the chiral pool using an amino acid building block to synthesize single (*S*,*R)*-eutomers (Scheme 2). The requisite (*R*)-THIQ ester **13** was prepared in gram-scale from commercially available 2-bromo-D-phenylalanine via a 6-step sequence comprising a Pictet-Spengler reaction and protecting group manipulations developed by Beadle *et al*.[28] Chiral HPLC analysis of **13** showed a good enantiomeric ratio (e.r. = 94:6).[29] Buchwald-Hartwig amination of **13** provided coupling product **14** with the retention of enantiopurity (e.r. = 93:7).[30] The conversion of ester **14** to aldehyde **15** via DIBAL-H reduction followed by reductive amination with (*S*)-5,6,7,8-tetrahydroquinolin-8-amine **16** gave the chiral-enriched amine **17** (d.r. = 12:1) which was utilized as an advanced intermediate to access a variety of side-chain modified analogues via reductive amination or *N*-

alkylation reactions. Treatments of **17** with appropriate electrophiles (aldehydes, ketones, alkyl bromides) under standard conditions afforded the penultimate Boc-protected intermediates **18a-h**, which were isolated as single diastereomers. Global Boc deprotection with TFA furnished target compounds **19a-h**.

Scheme 2. Side Chain Modifications[α]

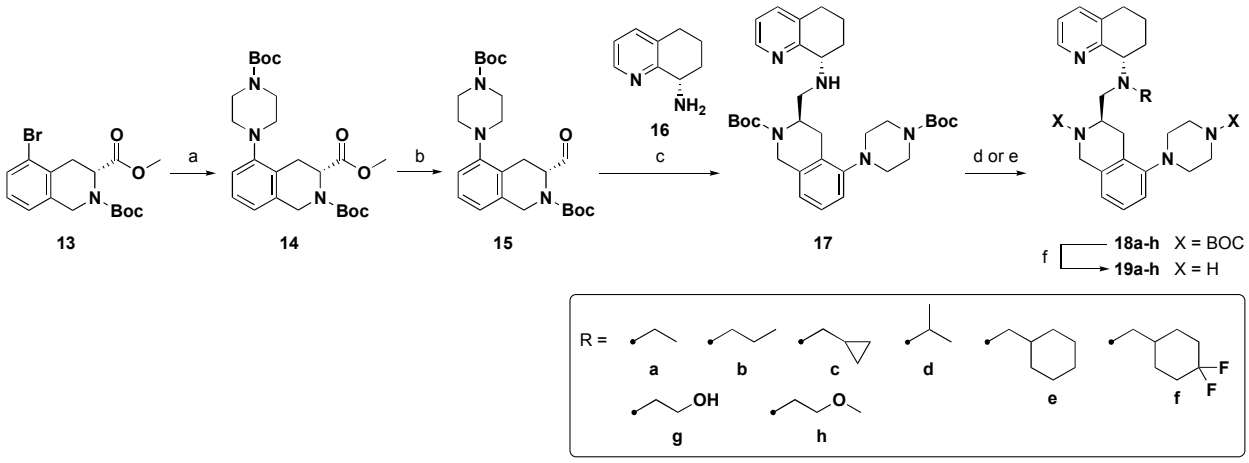

[α]Reagents and conditions: (a) 1-Boc-piperazine, $Pd_2(dba)_3$, (±)-BINAP, Cs_2CO_3, toluene, 120 ºC, sealed tube; (b) DIBAL-H, toluene, -78 ºC; (c) **16**, $NaBH(OAc)_3$, 1,2-DCE, rt; (d) aldehyde/ketone, $NaBH(OAc)_3$, 1,2-DCE, rt; (e) RBr, DIPEA, 1,2-DCE, 70 ºC; (f) TFA, DCM, rt.

All final compounds were profiled for inhibitory activity against CXCR4 and counter-screened against mAChR to determine the extent of off-target activity. In parallel with evaluating GPCR activities, the assessments of critical *in vitro* ADME parameters including metabolic stability, CYP450 inhibition, and passive permeability were also incorporated into the screening paradigm. To streamline the screening process, a high-throughput metabolic stability assay was employed in which we measured the percentage of test compound remaining after a 10-min incubation in liver microsome preparations.[31] For the passive permeability screen, we measured the permeation rate (P_c) of the test compound across a lipid-infused artificial membrane by the high-throughput PAMPA assay.[32] In addition, to minimize potential DDI risks, we routinely monitored the inhibitory activity of every compound against two primary drug-metabolizing

CYP isozymes (2D6 and 3A4). With this screening paradigm, we defined a target product profile with the following criteria: (1) potent CXCR4 antagonist activity ($IC_{50} \leq 100$ nM); (2) over 1000-fold CXCR4 selectivity versus mAChR; (3) >50% and >20% remaining in HLM and MLM; (4) clean CYP profile with all IC_{50} values greater than 20 μM; and (5) P_c greater than 100 nm/s.

Table 2. Effect of Varying Side Chains on Potency and In Vitro ADME Properties.

Compd	CXCR4 Ca^{2+} Flux IC_{50} (nM)[a,e]	mAChR Ca^{2+} Flux IC_{50} (μM)[f]	Microsomal Stability % remaining[b,f]		Inhibition of CYP450 3A4 IC_{50} (μM)[c,f]	Inhibition of CYP450 2D6 IC_{50} (μM)[c,f]	PAMPA permeability P_c (nm/s)[d,e]
			Human	Mouse			
12a	6.08±1.43	7.18	99.7	19.9	>20.0	>20.0	0
19a	14.8±3.98	8.60	79.1	53.8	>20.0	>20.0	75.0±14.0
19b	32.2±9.21	3.16	100	87.4	>20.0	12.0	26.5±16.0
19c	26.7±1.68	21.6	82.1	88.3	>20.0	8.57	87.0±18.0
19d	364±257	8.34	75.0	91.0	> 20.0	> 20.0	16.0[f]
19e	715±182	>33.3	81.6	85.6	1.78	5.72	9.00±13.0
19f	498±198	>33.3	68.6	76.6	5.62	8.45	0
19g	195±4.10	>33.3	94.4	60.3	> 20.0	> 20.0	11.0±2.00
19h	154±69.4	5.60	90.3	83.7	>20.0	14.2	1.00±2.00

[a]Concentration of compound inhibiting the CXCR4 Ca^{2+} flux/release by 50%, reported as the mean from two independent experiments (n=2). [b]Metabolic stability was determined as percentage of test compound remaining after incubation for 10 minutes at 37 °C in liver microsome preparations (CYP450 and other NADP-dependent enzymes). [c]The lower limit (< 20 μM) in the CYP450 assays (2D6 and 3A4) is shown. [d]Measured at pH 7.4. [e]n=2, reported error represents standard deviation. [f]n=1.

As illustrated in Table 2, the CXCR4 activity appeared to be quite sensitive to the length and size of the side chain. While the ethyl analogue **19a** was equipotent to the lead methyl compound **12a**, the *n*-Pr (**19b**) and *c*-$PrCH_2$ (**19c**) led to a 4-fold loss of potency. Sterically bulky substituents, such as *i*-Pr (**19d**), *c*-$HexCH_2$ (**19e**), or F_2-*c*-$HexCH_2$ (**19f**) dramatically reduced the potency (IC_{50} = 300-700 nM). This steep SAR strongly suggested that steric clashes of larger side chains with other substructures in the vicinity could alter the binding mode of the molecule to CXCR4. In tandem with hydrophobic attachments, we sought to engage additional H-bond donor/acceptors to pick up other interactions with the receptor by incorporating the hydroxyl

(**19g**) and methoxy (**19h**) groups to the terminal position of the ethyl side chain. However, these polar substituents were not well-tolerated, as they led to a 20-30-fold drop in potency. We surmised this erosion of activity was likely the result of electrostatic repulsion between the heteroatom on the side chain and the piperazine NH, given the close spatial proximity of these two moieties. Interestingly, the steric bulk of the side chain appeared to mitigate the mAChR activity as reflected by the following trend regarding the IC_{50} values Me (**12a**) ~ Et (**19a**) ~ iPr (**19d**) < *c*-$PrCH_2$ (**19c**) < *c*-$HexCH_2$ (**19e**). The presence of a heteroatom within the side chain (**19f**, **19g**) abolished the activity against this off-target receptor (IC_{50} > 30 μM). Within this set of analogues, the metabolic stability in MLM was generally improved as compared to **12a**, and these compounds were quite stable toward HLM (70-100% of original compounds remained after 10 min). Nevertheless, none of these analogues showed desirable P_c, and five out of the ten tested compounds, namely **19b**, **19c**, **19e**, **19f, 19h**, moderately inhibited CYP 2D6 isozyme. From these preliminary SAR, it is evident that none of the side chains in this survey surpassed the methyl group in terms of providing better CXCR4 potency, selectivity over mAChR, and ADME properties. As a result, we shifted our attention to the northern portion of the chemotype.

Instead of establishing an extensive round of SAR exploration, we decided to replace the THQ headpiece with selected 2-(aminomethyl)pyridine moieties, *e.g.*, 3-Me (**21a**) and 3,5-diMe (**21b**), which have been shown to improve the potency in the pyridyl series derived from the redesign of AMD11070.[33] As illustrated in Scheme 3, aldehyde **15** was utilized as the common starting material for the synthesis of headpiece-modified analogues. Reductive amination reactions of **15** with amines **S1** through **S4** produced Boc-protected intermediates **20a-d**. Subsequent treatment of these intermediates with TFA furnished final compounds **21a-d**.

Scheme 3. Headpiece Modifications[α]

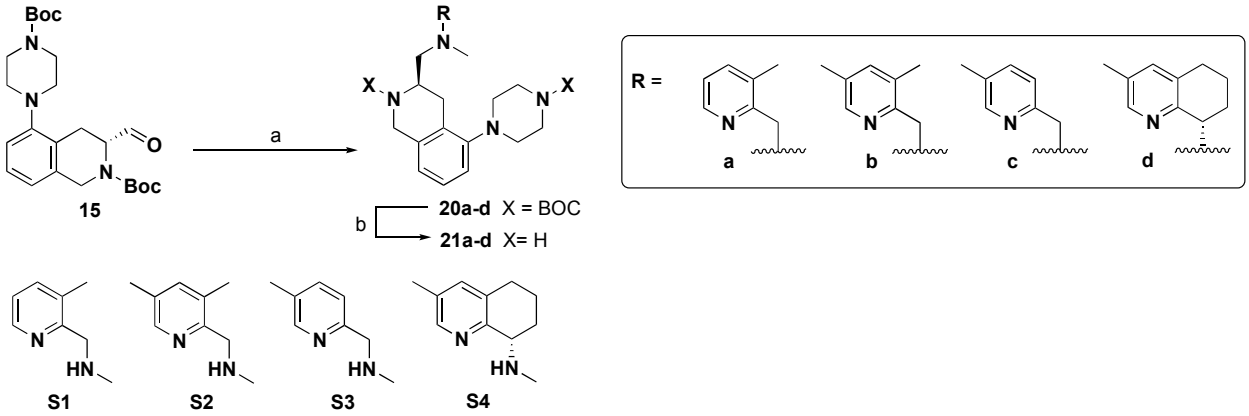

[a]Reagents and conditions: (a) amine (**S1**, **S2**, **S3, S4**), $NaBH(OAc)_3$, 1,2-DCE, rt; (b) TFA, DCM, rt.

Interestingly, the 'open chain' analogues (**21a-c**) turned out to be less potent than **12a** (Table 3). Although the 3,5-diMe analogue (**21b**) exhibited fairly potent CXCR4 activity (IC_{50} = 21.4 nM), deletion of the methyl group at C-3 on the pyridyl ring, exemplified by the 5-Me analogue (**21c**), resulted in a substantial loss (24-fold) of potency (IC_{50} = 510 nM), indicating substitution at C-3 on the pyridyl ring is required for activity. As was noted in a recent publication on the THIQ series,[22] exchanging the THQ headpiece with aforementioned pyridylmethyl moieties improved mouse metabolic stability, and in this set, this observation was corroborated. For example, compounds **21a** and **21c** showed an improvement (69% and 77%) with lower metabolic turnover in MLM as compared to **12a** (20%). However, none of these open chain analogues significantly diminished (**21a-c**: all IC_{50}'s <16 μM) the muscarinic activity of **12a**. In addition to 'open scaffold' headpieces, we also synthesized and tested an analogue bearing methyl substitution at C-5 on the THQ ring.[22] Compound **21d** showed a marginal decrease (2-3-fold) in CXCR4 activity relative to **12a** together with the obliteration of muscarinic activity (IC_{50} > 16.7 μM) and a modest improvement in MLM stability (2-fold), but failed to improve the PAMPA permeability. However, the loss of CXCR4 potency for all these analogues failed to distinguish these from **12a** in terms of the therapeutic index

(CXCR4/mAChR ratios). Therefore, other substitutions around the THQ core were not explored in this medicinal chemistry program. Collectively, these results, in conjunction with the SAR of the side chain, suggested that further improving the potency of **12a** might be very difficult to achieve. Therefore, our subsequent efforts were directed to optimizing the profile of **12a** via modifications in the southern region of the molecule, mainly on the piperazine ring.

Table 3. SAR of the Northern Region.

Compd	CXCR4 Ca^{2+} Flux IC_{50} (nM)[a,f]	mAChR Ca^{2+} Flux IC_{50} (μM)[g]	Microsomal Stability % remaining[b,g]		Inhibition of CYP450 3A4 IC_{50} (μM)[c,g]	PAMPA permeability P_c (nm/s)[d,f]
			Human	Mouse		
12a	6.08±1.43	7.18	99.7	19.9	>20.0	0
21a	91.2±12.2	11.1	100	69.2	1.42	193±61.5
21b	21.4±3.67	15.4	100	ND[e]	>20.0	0
21c	510±234	9.56	100	76.8	>20.0	225±26.0
21d	16.1±6.33[h]	>16.7	100	47.8	>20.0	9.00±13.0
35	25.2±11.0[i]	>16.7	67.8	43.5	>20.0	323[g]

[a]Concentration of compound inhibiting the CXCR4 Ca^{2+} flux/release by 50%, reported as the mean from two independent experiments (n=2) unless otherwise stated. [b]Metabolic stability was determined as percentage of test compound remaining after incubation for 10 minutes at 37 °C in liver microsome preparations (CYP450 and other NADP-dependent enzymes). [c]The lower limit (< 20 µM) in the CYP450 assays (2D6 and 3A4) is shown; all compounds had >20 μM activity against CYP 2D6. [d]Measured at pH 7.4. [e]ND = not determined. [f]n=2, reported error represents standard deviation. [g]n=1. [h]n=3, reported error represents standard deviation. [i]n=4, reported error represents standard deviation.

Lead Optimization Process. As described previously, the two main liabilities in the pharmacological profile of **12a** included the weak inhibition of mAChR and poor PAMPA permeability. Since the latter dictates the oral bioavailability which was deemed an important property in this medicinal chemistry program, increasing the permeability became a priority. We suspected that the intermediate lipophilicity (cLogP 2.97),[34] two H-bond donors, and basic amine centers in the southern quadrants of the chemotype were contributors to the insufficient passive permeability by not allowing sufficient population of the free-base form.

From a medicinal chemistry perspective, the synthetic route detailed in Scheme 1 was not amenable for iterative cycles of design, synthesis, and evaluation of piperazine-modified

analogues since functionalizing the THIQ ring at an early stage requires cumbersome tasks of purification and characterization of intermediates. In a search for an alternative route to accelerate the lead optimization process, we devised a robust diversity-oriented strategy by reordering synthetic steps to generate molecular diversity at the penultimate step via a "late-stage" Buchwald-Hartwig amination (Scheme 4). The revised route started with a DIBAL-H reduction, which converted ester **13** to the corresponding aldehyde **22**. Subsequent reductive amination of **22** with amine **10** furnished the bromide **23**. This two-step sequence allowed us to prepare gram quantities of the key intermediate **23**, which was subjected to Buchwald-Hartwig couplings with a variety of commercially available piperazine derivatives, followed by TFA-mediated *N*-Boc cleavage to readily deliver desired targets **25a-p**.

Scheme 4. Piperazine Modifications via Late Stage Buchwald-Hartwig Coupling[α]

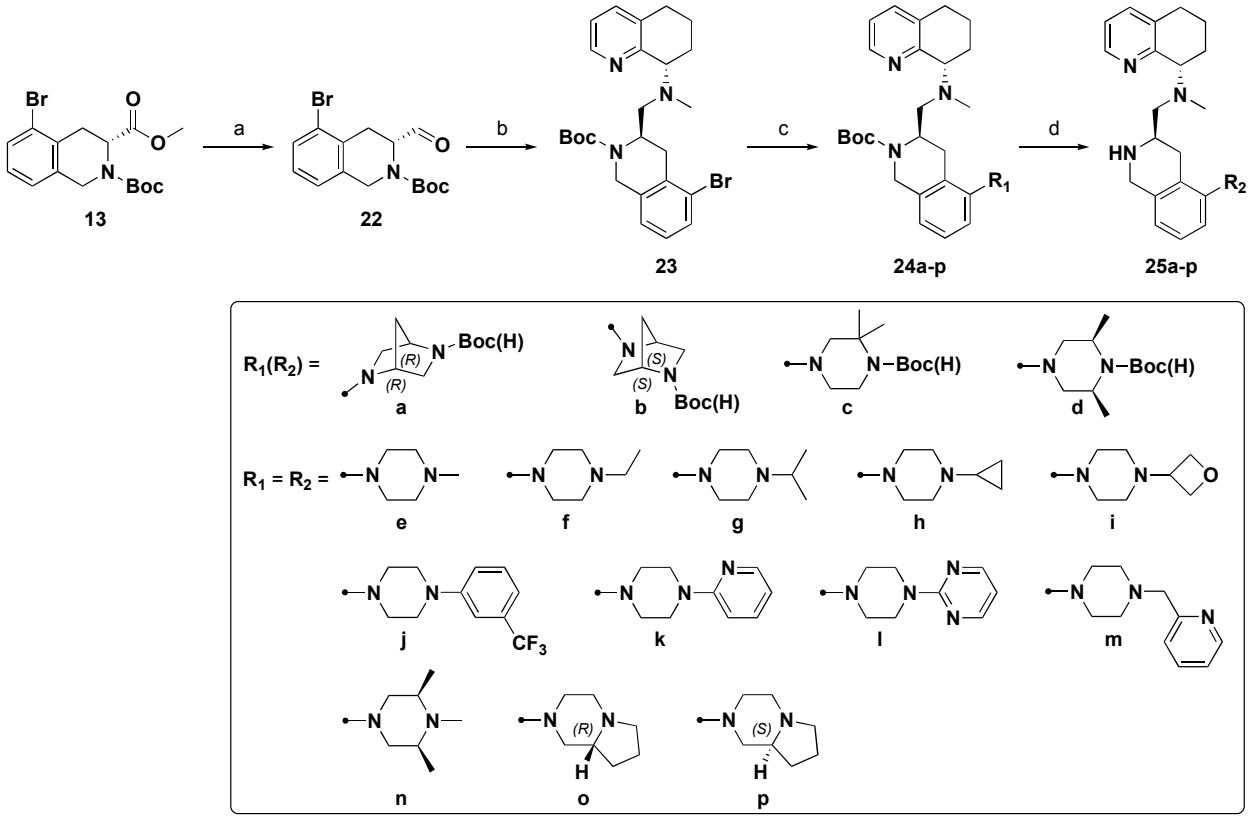

[α]Reagents and conditions: (a) DIBAL-H, toluene, -78 ºC; (b) **10**, $NaBH(OAc)_3$, 1,2-DCE, rt; (c) amine, $Pd_2(dba)_3$, (±)-BINAP, Cs_2CO_3, toluene, 120 ºC, sealed tube; (d) TFA, DCM, rt.

Our first approach to improve the permeability involved the inclusion of small hydrophobic moieties into the piperazine core to increase the lipophilicity and modulate the basicity. As summarized in Table 4, the addition of a carbon bridgehead or a *gem*-dimethyl substituent into the piperazine ring (**25a-c**), which was anticipated to reduce the basicity (pK_a) of the piperazine nitrogen by inducing additional steric interactions with the putative ammonium ion, did not have substantial impact in the PAMPA assay (P_c = 0 nm/s). However, compound **25a** did have a great improvement observed in both the muscarinic and MLM properties despite being 3-4 fold less potent in the calcium flux assay. Interestingly, the stereoisomer **25b** had over 20-fold loss in CXCR4 potency compared to **12a** and was 7-fold less potent than **25a**. Introduction of methyl groups to both sides of the piperazine NH in **25d** further elevated *c*LogP (3.81) but only resulted in a modest improvement in permeability (P_c = 39 nm/s) along with a 10-fold reduction in CXCR4 potency versus **12a**. However, improvements in muscarinic and MLM properties were observed similar to **25a**. At this juncture, further changes in the piperazine ring structure were not considered, as not only was CXCR4 potency affected negatively but also the permeability increase was not realized. In addition, since the *c*LogP values were increasing, we considered the observation that highly lipophilic compounds are generally associated with increased promiscuity, high plasma protein binding, and potent *h*ERG inhibition would be steering us in the wrong direction.[35]

Table 4. SAR of the Southern Quadrants

Compound	CXCR4 Ca^{2+} Flux IC_{50} (nM)[a,f]	mAChR Ca^{2+} Flux IC_{50} (μM)[g]	Microsomal Stability % remaining[b,g]		Inhibition of CYP450 3A4 IC_{50} (μM)[c,g]	Inhibition of CYP450 2D6 IC_{50} (μM)[c,g]	PAMPA permeability P_c (nm/s)[d,f]
			Human	Mouse			
12a	6.08±1.43	7.18	99.7	19.9	>20.0	>20.0	0
25a	20.7±9.21[h]	>16.7	100	95.9	>20.0	>20.0	0

25b	146±83.0	>16.7	100	36.3	>20.0	>20.0	0
25c	33.9±26.0	17.9	100	44.0	>20.0	>20.0	0
25d	61.0±45.8	>33.3	100	85.6	>20.0	>20.0	39.0±56.0
25e	29.6±15.7	>33.3	75.8	17.0	>20.0	>20.0	996±11.0
25f	13.8+5.45[h]	>33.3	0	18.8	>20.0	>20.0	205[g]
25g	16.9±9.51[h]	>16.7	56.6	15.1	>20.0	8.13	143±13.0
25h	23.5±9.16[h]	>33.3	15.5	7.00	4.23	6.09	265±2.00
25i	381±355	>16.7	83.1	50.8	>20.0	>20.0	725±170
25j	>16,700	9.25	90.3	72.3	2.21	6.48	141±12.5
25k	17.9[g]	1.98	27.4	46.1	3.16	2.52	129±26.0[e]
25l	30.7±16.8	0.887	35.5	35.1	3.35	0.508	360±65.0[e]
25m	4.47±3.29	10.8	4.20	40.4	6.79	11.0	82.0±32.0[e]
25n	14.1±2.57[h]	15.1	24.6	39.6	>20.0	>20.0	142±31.0
25o	3.59[g]	26.1	52.2	36.7	>20.0	>20.0	740±481
25p	2.92±1.93	>16.7	36.6	40.1	>20.0	>20.0	167[g]
29	32.0±16.6[h]	26.3	100	100	>20.0	>20.0	3.00±4.00
30	171±142	>16.7	83.3	41.7	>20.0	>20.0	364±39.0

[a]Concentration of compound inhibiting the CXCR4 Ca^{2+} flux/release by 50%, reported as the mean from two independent experiments (*n*=2) unless otherwise stated. [b]Metabolic stability was determined as percentage of test compound remaining after incubation for 10 minutes at 37 °C in liver microsome preparations (CYP450 and other NADP-dependent enzymes). [c]The lower limit (< 20 μM) in the CYP450 assays (2D6 and 3A4) is shown. [d]Measured at pH 7.4. [e]Measured at pH 5.5. [f]n=2, reported error represents standard deviation. [g]n=1. [h]n=4, reported error represents standard deviation.

Consequently, we turned our attention to the second approach in which we envisaged reducing the number of HBD counts by grafting a methyl group onto the distal piperazine nitrogen, which has been shown to improve passive permeability.[36] Accordingly, we made the *N*-methyl analogue **25e**. As predicted, this modification resulted in a substantial improvement in permeability (P_c = 996 nm/s), albeit at the expense of a marginal, 5-fold, reduction in CXCR4 potency (IC_{50} = 29.6 nM) and a small reduction in human microsomal stability. Gratifyingly, the CYP profile remained intact, as no inhibitory potential was observed toward recombinant CYP enzymes. This modification has proven to be particularly advantageous for the selectivity over off-targets as compound **25e** was completely devoid of mAChR activity (IC_{50} > 30 μM). These observations hence encouraged us to also probe the impact of removing the HBD on the THIQ ring. Scheme 5 illustrated our synthetic efforts on capping the THIQ nitrogen with a methyl

group. A Cbz-protected piperazine moiety was coupled to compound **23** to provide the orthogonally protected intermediate **26**. Cleavage of the *N*-Boc group by TFA gave **27**, which underwent reductive amination with formalin to furnish **28**. Removal of the Cbz protecting group by treatment with trifluoromethanesulfonic acid yielded compound **29**. Of note, efforts to cleave the *N*-Cbz group via canonical Pd-catalyzed hydrogenolytic conditions were unsuccessful, presumably due to the high basicity of the compound.

Scheme 5. Methylation of THIQ Nitrogen[α]

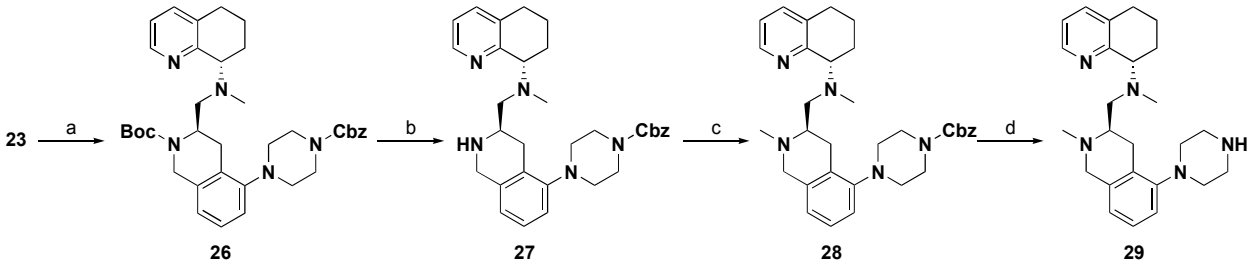

[α]Reagents and conditions: (a) 1-Cbz-Piperazine, $Pd_2(dba)_3$, (±)-BINAP, Cs_2CO_3, toluene, 120 ºC, sealed tube; (b) TFA, DCM, rt; (c) paraformaldehyde, $NaBH(OAc)_3$, 1,2-DCE, rt; (d) TfOH, TFA, rt.

Compound **29** with a methyl-decorated THIQ ring was ~5-fold less active than its *des*-methyl counterpart **12a**, with an IC_{50} of 32.0 nM versus 6.1 nM, respectively. Surprisingly, there was no boost in permeability, and this compound displayed exceptional stability in liver microsomes across all species as well as a large decrease in muscarinic activity. In light of this result, we envisioned that methylation of the THIQ ring NH in analogue **25e** would fine-tune its metabolic profile without compromising the CXCR4 activity, given that both methyl analogues **25e** and **29** possessed equivalent potency. With this idea in mind, we subjected the parent compound **12a** to a reductive amination conditions with excess paraformaldehyde to provide compound **30** (Scheme 1). As expected, the resulting analogue **30** showed an additive improvement in metabolic stability (76 → 83% in HLM, 17 → 42% in MLM) compared to the N-methyl piperazine analog **25e**. However, compound **30** exhibited only moderate CXCR4

potency (IC_{50} = 171.1 nM) vis-à-vis being 5-6 fold less active than its counterparts (**25e**, **29**). It is interesting to note in this series that both compounds with the *N*-methyl piperazine nitrogen (**25e** and **30**) had superior permeability by >100-fold versus the THIQ *N*-methyl compound **29** in the PAMPA assay. This result in itself, points to the major role of the distal piperazine nitrogen in improving the basicity and also points to the direction and focus that future modifications should involve modified and *N*-alkylated piperazines.

As part of the effort to improve the microsomal stability of **25e**, we replaced the THQ headpiece with the tricyclic octahydrophenanthroline motif, which has been shown to reduce clearance and improve metabolic half-life.[19a] The phenanthroline analogue was synthesized by following similar methodology described in Scheme 1 using the (*R*)-TIQ ester **13** and 1-methylpiperazine for the Buchwald-Hartwig amination (Scheme 6). The resulting coupling product **31** was then converted to aldehyde **32** via DIBAL-H reduction. Reaction of **32** with amine **33** under reductive alkylation conditions and subsequent treatment of Boc-protected intermediate **34** with TFA furnished **35**. Profiling of **35** showed only modest improvement in MLM stability while the other attributes appeared to be comparable to those of **25e**. Taken together, it was evident that, at this point, only **25e** and **35** were capable of addressing both the off-target and permeability issues of **12a** while still maintaining potent CXCR4 antagonist activity, acceptable clearance, and a clean CYP profile. Given the long synthetic sequence required for the synthesis of the tricyclic headpiece and the observation that this group did not provide any additional *in vitro* improvements, we decided to pursue **25e** as the new lead for subsequent SAR exploration.

Scheme 6. Replacing THQ Headpiece with Tricyclic Octahydrophenanthroline Core[a]

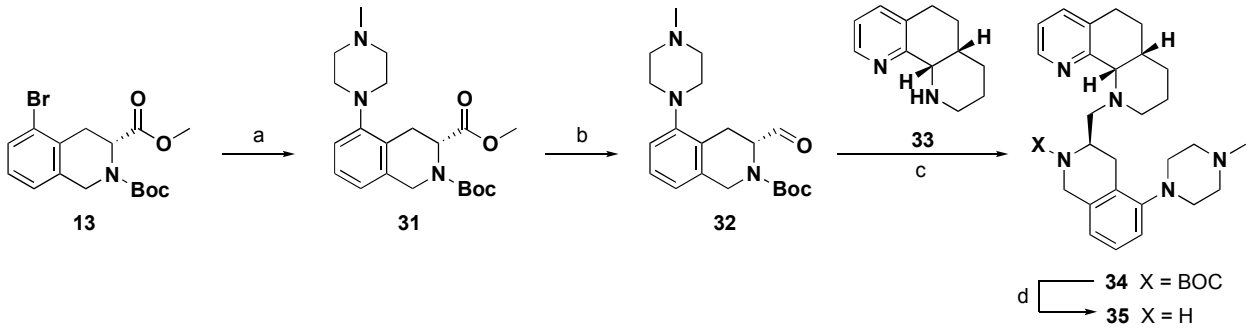

[a]Reagents and conditions: (a) 1-methylpiperazine, $Pd_2(dba)_3$, (±)-BINAP, Cs_2CO_3, toluene, 120 ºC, sealed tube; (b) DIBAL-H, toluene, -78 ºC; (c) **33**, $NaBH(OAc)_3$, 1,2-DCE, rt; (d) TFA, DCM, rt.

While compound **25e** was an attractive candidate for *in vivo* preclinical characterization, we still wanted to improve upon several features to enhance its drug-like properties. In particular, we wished to further increase its CXCR4 potency and microsomal stability while maintaining the permeability, clean CYP profile, and selectivity over mAChR. To this end, we focused on replacing the methyl group on the terminal piperazine nitrogen with a handful of substitutions possessing different size, steric demands, and electronic properties. As listed in Table 4, the first subset of analogues (**25f-h**) consisted of small aliphatic and alicyclic groups varying from ethyl to cyclopropyl. In general, these substituents provided analogues with desirable P_c and potent CXCR4 activity. Suspecting demethylation was the major liability, we considered a variety of replacements for this methyl. The ethyl analogue **25f** demonstrated a similar pharmacological profile to that of **25e**, with the exception of very low human liver metabolic stability. However, the *i*-Pr (**25g**) and *c*-Pr (**25h**) substituents somehow elicited a detrimental effect on metabolic stability, and these compounds also picked up moderate CYP 2D6 inhibition. The oxetanyl group (**25i**), which is well-known in medicinal chemistry for improving metabolic stability,[37] elicited a very attractive ADME profile but rendered the compound considerably less active against CXCR4 (10-fold, IC_{50} = 380 nM).

In the next set of analogues, we subtly changed the electronic nature of the appended substituent by utilizing electron-withdrawing aryl and heteroaryl groups (**25j-m**). Of this cohort, compounds **25k**, **25l**, **25m** were fairly permeable. Regarding CXCR4 potency, these substituents conferred good activity as relative to **25e**. This finding, in conjunction with the relatively flat SAR of aliphatic congeners, signified that the basicity and steric environment on this nitrogen may not be important for abrogating CXCL12-mediated receptor signaling. The only exception was the *m*-trifluoromethylphenyl analogue **25j**, which did not inhibit CXCR4 signaling at concentrations up to 17 μM. This might be the result of an electrostatic repulsion between fluorine atoms and the negatively charged side chains of aspartic or glutamic acid residues located in the extracellular binding regions of CXCR4. Perhaps not surprisingly, we encountered serious metabolic liabilities for heteroaryl variations which could be attributed to the properties inherent to the unadorned pyridine-like substructures. For example, the 2-pyridyl analogue **25k** inhibited mAChR, CYP 2D6, and 3A4 at low micromolar concentrations. The effect was much more profound in pyrimidyl congener **25l**, which is a potent mAChR and CYP2D6 inhibitor. Homologation of the 2-pyridyl moiety, as found in analogue **25m**, appeared to mitigate some of the aforementioned liabilities and reestablished a single-digit nanomolar on-target potency (IC_{50} = 4.5 nM). Despite these improvements, this compound was rapidly metabolized by HLM with only 4% of the original compound remaining at 10 min, thereby precluding it from further consideration. These SAR studies suggested that small aliphatic substituents, such as the methyl and ethyl, were preferred for the optimal balance of good activity and ADME properties.

The focus of this work then moved on to the identification of alternative piperazine cores that could lead to superior overall pharmacological profiles. Guided by the SAR findings from the preceding array of analogues, we elected to optimize **25d** in a rational, structure-based

fashion. The most obvious limitation of **25d** was the low permeability (P_c = 39 nm/s), which instantly prompted us to methylate the piperazine NH. As exemplified by the 3,4,5-trimethylpiperazine **25n**, this modification resulted in a moderate jump in permeability (P_c = 142 nm/s), together with a concomitant, 4-fold, increase in CXCR4 potency (IC_{50} = 14.1 nM). Of note, **25n** picked up some muscarinic activity (IC_{50} = 15 μM) but still remained >1000 fold selective for CXCR4. Of greater concern was that **25n** had a higher turnover rate in HLM (only 25% remaining after 10 min) than its *N*-*des*-methyl counterpart **25d**, suggesting *N*-demethylation is the major biotransformation. To address this issue, we judiciously deployed bicyclic piperazine moieties (**25o**, **25p**) as replacements for the 3,4,5-trimethylpiperazine. We reasoned that the pyrrolidine portion of these bicyclic piperazines would: (1) mask the *N*-methyl metabolic soft spot; (2) rigidify the piperazine ring; and (3) add lipophilicity to the molecule. Therefore, this modification may allow access to a more potent compound with improvements in clearance, selectivity, and permeability. Fortuitously, this idea proved successful as the loss in human microsomal stability was somewhat rescued by this modification, most notably in the *R*-congener **25o** (25 → 52% remaining). The lower clearance rate of **25o** versus **25e** was greatly outweighed by other improvements. For instance, **25o** featured an excellent CXCR4 potency (IC_{50} = 3.6 nM), large selectivity window (>5000-fold) over mAChR, high permeability (P_c = 740 nm/s), and a clean CYP profile. While the *S*-congener **25p** possesses equipotent CXCR4 activity (IC_{50} = 2.9 nM), its metabolic stability in HLM appeared slightly inferior to that of **25o** albeit a small difference. On the basis of these results, **25o** was deemed to have the best overall balance of properties and thus could be selected for further profiling of pharmacokinetic (PK), pharmacology, and safety characteristics in the future.

To get a better idea of the potential binding modes of these second-generation antagonists, we performed docking studies within the CXCR4 receptor. For this study, we chose TIQ15 and compound **25o** and utilized the IT1t:CXCR4 crystal structure (3ODU) to determine interactions within the receptor.[41] Overall, we found that **25o** picked up similar interactions to TIQ15 but with subtle differences (Figure 4). Most notably, how the shift in side chain attachment between the two molecules can allow similar positioning of hydrogen bond elements within the binding pocket. First we replicated the previous study with TIQ15 within CXCR4 showing that this molecule picked up key ionic interactions in the form of salt bridges with residues GLU 288 and ASP 97 as well as secondary interactions with the aromatic residues TRP 94, HIS 113 and TYR 116.[21c] Compound **25o** also picked up these salt bridges with the piperazine distal nitrogen to GLU 288 similar to the butyl amine chain of TIQ15. The homologous tetrahydroquinoline ring maintains aromatic interactions with TRP 94, HIS 113, and TYR 116 in both molecular configurations. The main difference seems to be positioning of the tetarhydroisoquinoline rings, with an approximate 90 degree difference in the plane of these ring systems. This difference is mainly due to the restriction of the butyl amine side chain to the bicyclic pieprazine to the 2-position of the ring. However, in both molecules, the THIQ ring still maintains the salt bridge to ASP 97.

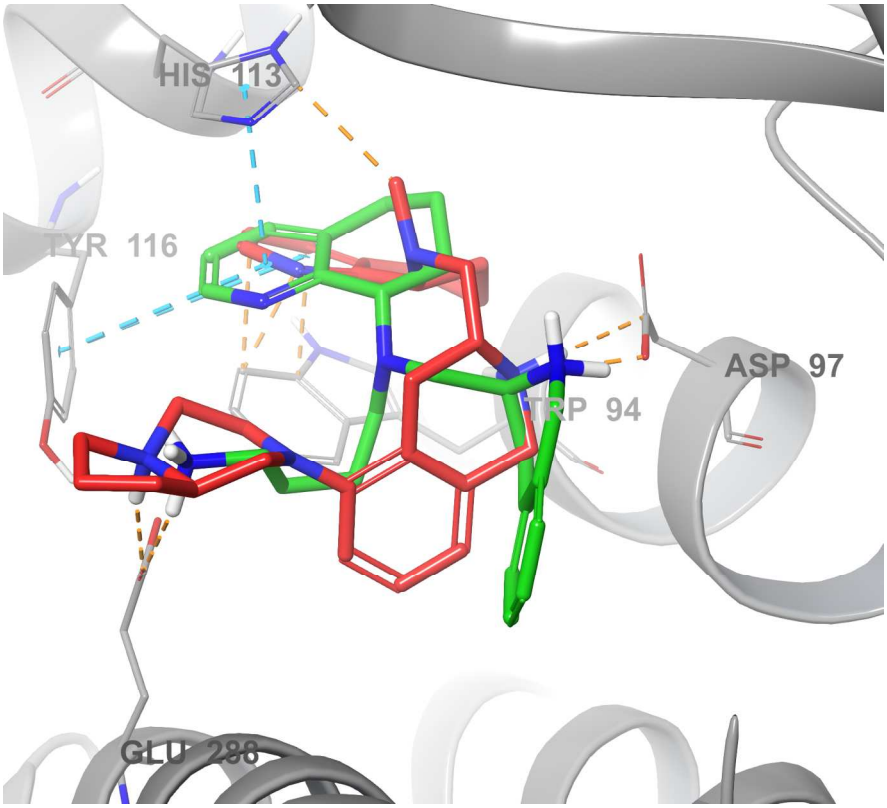

Figure 4. Docking Poses of TIQ15 (green) and compound **25o** (red) within the 3ODU crystal structure. Key residues are labeled in light gray (ASP 97, TRP 94, HIS 113, TYR 116 and GLU 288).

CONCLUSIONS

In summary, we have successfully redesigned our previously reported THIQ chemotype in an effort to address the poor mouse microsomal stability, potent CYP 2D6 inhibition, and poor predicted intestinal permeability. Structural alterations of the parent compound TIQ15 gave rise to an equipotent analogue **12a**, which exhibited improved metabolic stability and substantial reduction of inhibition against CYP 2D6. However, **12a** demonstrated weak mAChR activity in a calcium flux counterscreen and low intestinal permeability in the PAMPA assay. Facilitated by efficient Buchwald-Hartwig coupling and the commercial availability of structurally-diverse piperazine building blocks, the SAR of **12a** was explored through the preparation of 32

analogues that examined the headpiece, side chain, and the piperazinyltetrahydroisoquinoline core. Subsequent optimization of **12a** resulted in the identification of compound **25o**, which demonstrated superb on-target potency in combination with favorable *in vitro* ADME properties, including reduced mAChR activity and enhanced permeability. Further *in vitro* and *in vivo* safety and pharmacokinetics studies of **25o** are currently underway and will be reported in due course.

EXPERIMENTAL SECTION

CXCR4 and Muscarinic Receptor Calcium Flux Assays. The compounds were tested for their ability to induce or inhibit calcium flux in CCRF-CEM cells. The experimental procedure and results are provided below. The exemplified biological assays, which follow, have been carried out with all compounds. Human T lymphoblast cells (CCRF-CEM) expressing endogenous CXCR4 receptors and muscarinic acetylcholine receptors were grown in suspension culture and plated in clear bottom 384-well microplates (Greiner bio-one Cat# 789146) in assay buffer [Hank's Buffered Saline Solution (Gibco Cat# 14025-092) supplemented with 20 mM HEPES (Gibco Cat# 15630-080) and 0.1% fatty-acid free BSA (Sigma Cat# A9205)] at 40,000 cells per well. The cells were loaded with equal volume of calcium indicator dye (AAT Bioquest Inc, Cat# 34601) for 30 minutes at 37°C. The cells were then equilibrated to room temperature for 15 minutes before assay. Test compounds solubilized and serially diluted in DMSO were transferred to 384 well plates (Matrix Cat# 4307). The serially diluted compounds were diluted to working concentrations with the same assay buffer to 0.5% DMSO. They were added to the cells by FDSS6000 (Hamamatsu) at final concentrations ranging from 25,000 nM to 0.423 nM. Activity of the compounds to induce calcium flux was monitored by FDSS in the "agonist mode" for 90

sec. For "antagonist mode" assessment, the cells are subsequently incubated for 25 minutes at room temperature. SDF-1α (R&D System Cat# 350-NS/CF) or acetylcholine was then added at a final concentration of 5 nM and 2,000 nM, respectively, to stimulate the cells. Inhibition of SDF-1α and acetylcholine-induced calcium flux was monitored by FDSS6000 for 90 seconds. Activation data for the test compound over a range of concentrations was plotted as percentage activation of the test compound (100% = maximum response triggered by a saturating concentration of SDF-1α, *i.e.*, 160 nM). After correcting for background, EC_{50} values were determined. The EC_{50} is defined as the concentration of test compound, which produced 50% of the maximal response and was quantified using the 4-parameter logistic equation to fit the data. Inhibition data for the test compound over a range of concentrations was plotted as percentage inhibition of the test compound as compared to an internal control compound. The IC_{50} is defined as the concentration of test compound, which inhibits 50% of the maximal response and was quantified using the 4-parameter logistic equation to fit the data. None of the compounds tested demonstrated agonist activity in the calcium flux assay. All compounds demonstrated EC_{50} values >30 μM. In contrast, compounds demonstrated a range of potencies in inhibiting SDF-1α -induced calcium flux. For the CXCR4 assay, most compounds were tested in replicate in two separate experiments except where noted in the tables. For compounds **25k** and **25o** there was only one experiment in replicate. For compound **21d** there were three separate experiments. For compounds **25a**, **25f-h**, **25n**, **29** and **35** there were four separate experiments in replicate conducted. For the mAChR assay, results reported are in duplicate from a single experiment for all compounds.

PAMPA Assay. Compounds and controls are utilized as 10 mM stocks in 100% DMSO. Compounds are diluted 1:100 in pH 7.4 or pH 5.5 donor well buffer (pION CAT # 110151) providing a 100 μM assay solution in 1% DMSO. Compound diluted in donor well buffer is transferred to a Whatman Unifilter plate and filtered prior to dispensing 200 μL into the donor well of the assay plate (pION CAT #110163). The PAMPA membrane is formed by pipetting 4 μL of the lipid solution (pION CAT #110169) onto the filter plate (VWR CAT #13503). The membrane is then covered with 200 μL of acceptor well buffer at pH 7.4 (pION CAT #110139). The PAMPA assay plate (donor side and acceptor side) is combined and allowed to incubate at room temperature for 4 hours. The plate is then disassembled and spectrophotometer plates (VWR CAT #655801) are filled (150 μL/well). The donor, acceptor, reference, and blank plates are read in the SpectraMax UV plate reader. Data is captured by the pION software which analyzes the spectra and generates P_c values. Each compound was tested in duplicate in two independent experiments except where noted in the tables. For compounds **19d**, **25f**, **25p** and **35** only one experiment in duplicate was performed.

Recombinant CYP2D6 Inhibition Assay. The CYP2D6 inhibition assay utilizes microsomes from the insect cells expressing human recombinant CYP2D6 enzyme and fluorogenic probe (AMMC, 3-[2-(*N*,*N*-diethyl-*N*-methylamino)ethyl]-7-methoxy-4-methylcoumarin) that produces fluorescent metabolite; both reagents were obtained from Thermo Fisher Scientific/Discovery Labware (Woburn, MA). Assay was performed in 1536-well microplates in a total volume of 5 µl. Automated liquid handling equipment (Thermo Multidrop Combi, LabCyte ECHO 550) was used in all steps of compound preparation and for assay reagent additions. Each compound was tested in duplicate at 7 concentrations ranging from 1 nM to 20 μM; final concentration of DMSO in reactions was 0.2%. Positive controls were included in each experiment/run. Test

compounds (10 nL/well) were first pre-incubated at 37°C for 30 min with 2.5 μL of prewarmed 2-fold-concentrated mixture of AMMC fluorogenic substrate (3 μM) and 12.5 nM rCYP2D6 enzyme in 100 mM potassium phosphate assay buffer pH 7.4. At the end of preincubation, the reactions were initiated by the addition of 2.5 μL of prewarmed 2-fold-concentrated NADPH-regenerating system (16.2 nM NADP) in the same assay buffer. Assay plates were then incubated at 37°C for 45 min. Following incubation, reactions were terminated by the addition of 3 μL of quench buffer (80% acetonitrile, 20% 0.5 M TRIS-base). Fluorescence intensity was measured using the Envision fluorescence plate reader (Perkin Elmer) at excitation and emission wavelengths of 405 and 460 nm, respectively, using a 430-nm cut-off filter. The end-point fluorescence readout was normalized to the fluorescence intensity of the reaction performed in the absence of the test substance (totals, 0% inhibition) and the mixture of reaction components in the presence of "Inhibitor Cocktail" (background, 100% inhibition). The IC_{50} value for each compound is derived from the fitted 20-point curve using a four-parameter logistic regression model. Each compound was tested in duplicate in a single experiment.

Metabolic Stability Assay. The metabolic stability of final compounds was determined in human and mouse liver microsomes using the compound depletion approach in single experiments, quantified by LC/MS/MS described previously.[38] Each compound was tested in duplicate in a single experiment.

General. All solvents and reagents were purchased from commercial suppliers and used without further purification. Analytical thin layer chromatography was carried out on silica pre-coated glass plates Merck KGaA (silica gel 60 F_{254}, 0.25 mm thickness) and visualized with UV light at 254 nm and/or with phosphomolybdic acid, idodine. Automated flash chromatography was performed on Teledyne ISCO CombiFlash R_f 200 system with RediSep R_f prepacked silica

cartridges (60 Å, 40-63 μm particle-size). Concentration refers to rotary evaporation under reduced pressure.

^{1}H, ^{13}C, ^{19}F NMR spectra were recorded on Varian INOVA or VNMR spectrometer operating at 400 MHz at ambient temperature with $CDCl_3$ or methanol-d_4 as solvents. Data for ^{1}H NMR were recorded as follows: δ chemical shift (ppm), multiplicity (s, singlet; d, doublet; dd = doublet of doublet; t, triplet; q, quartet; m, multiplet; br, broad; etc.), coupling constant (Hz), integration. Chemical shifts are reported in parts per million relative to internal reference $CDCl_3$ (^{1}H NMR: δ 7.26; ^{13}C NMR: δ 77.16), methanol-d_4 (^{1}H NMR, δ 4.87, 3.31; ^{13}C NMR, δ 49.00), TMS (^{1}H NMR: δ 0.00), or external reference TFA (^{19}F NMR: δ -76.55 ppm).

Liquid chromatography/mass spectrometry (LCMS) data was obtained to verify molecular mass and analyze purity of products. The specifications of the LCMS instrument are the following: Agilent 1200 HPLC coupled to a 6120 quadrupole mass spectrometer (ESI-API), UV detection at 254 and 210 nm, Agilent Zorbax XDB-18 C_{18} column (50 mm x 4.6 mm, 3.5 µm), gradient mobile phase consisting of MeOH/water/0.1 % formic acid buffer, and a flow rate of 1.00 mL/min. The chemical purity of all final compounds was determined by LCMS and confirmed to be $\geq$ 95%.

Normal phase analytical chiral HPLC was performed on Agilent 1100 HPLC equipped with G1315B diode array detector using mixtures of hexanes/IPA and Daicel ChiralPak AD-H column (150 mm x 4.6 mm, 5 μM). Reverse phase HPLC was performed on the same instrument using mixtures of MeCN/H_2O and Daicel ChiralCel OD-RH column (150 mm x 4.6 mm, 5 μM). High resolution mass-spectra (HRMS) were acquired on a VG 70-S Nier Johnson or JEOL mass spectrometer.

The following compounds were prepared according to reported protocols: (*S*)-*N*-methyl-5,6,7,8-

tetrahydroquinolin-8-amine (**10**),[39] (*S*)-5,6,7,8-tetrahydroquinolin-8-amine (**16**),[40] (*R*)-2-tert-butyl 3-methyl 5-bromo-3,4-dihydroisoquinoline-2,3(1*H*)-dicarboxylate (**13**),[28] 1,2,3,4,4a,5,6,10b-octahydro-1,10-phenanthroline (**33**).[19a]

The synthesis, characterization data, and associated references for the following compounds are provided in the Supporting Information: *N*-methyl-1-(3-methylpyridin-2-yl)methanamine (**S1**), 1-(3,5-dimethylpyridin-2-yl)-*N*-methylmethanamine (**S2**), , *N*-methyl-1-(5-methylpyridin-2-yl)methanamine (**S3**), (*S*)-3-methyl-5,6,7,8-tetrahydroquinolin-8-amine (**S4**).

Synthesis

2-(tert-Butyl) 3-methyl 5-bromo-3,4-dihydroisoquinoline-2,3(1H)-dicarboxylate (**7**). To a 250-mL round-bottom flask was charged with methyl 5-bromo-1,2,3,4-tetrahydroisoquinoline-3-carboxylate HCl salt (3.0 g, 9.79 mmol), 1,4-dioxane (100 mL), and saturated sodium bicarbonate solution (100 mL). Di-tert-butyl dicarbonate (4.27 g, 19.6 mmol) was added at room temperature. The biphasic mixture was stirred for 90 minutes and then transferred to a separatory funnel and extracted twice with ethyl acetate. The combined organic extract was dried over anhydrous sodium sulfate and concentrated under reduced pressure to a crude material which was purified by CombiFlash system (40g silica column, 5 minutes hexanes → 30 minutes 0-20% EtOAc/hexanes) to afford the title compound as a clear gum (3.50 g, 96 % yield). ^{1}H NMR (400 MHz, $CDCl_3$): δ 7.42 (t, J = 4.6 Hz, 1H), 7.18 - 6.89 (m, 2H), 5.20 (dd, J = 6.9, 2.6 Hz, 0.5H), 4.89 - 4.60 (m, 1.5H), 4.48 (dd, J = 29.2, 16.6 Hz, 1H), 3.65 (d, J = 10.9 Hz, 3H), 3.46 (ddd, J = 56.7, 16.5, 3.5 Hz, 1H), 3.08 (ddd, J = 48.9, 16.6, 6.7 Hz, 1H), 1.49 (d, J = 23.9 Hz, 9H). HRMS (*m/z*): calculated for $[C_{16}H_{20}BrNO_4 + H]^+$: 370.06540, found: 370.06521.

2-tert-butyl 3-methyl 5-(4-(tert-butoxycarbonyl)piperazin-1-yl)-3,4-dihydroisoquinoline-2,3(1H)-dicarboxylate (**8**). To an oven-dried Biotage 10-20 mL microwave vial equipped with a magnetic

stir bar was charged with ester **7** (1.03 g, 2.78 mmol), tert-butyl piperazine-1-carboxylate (622 mg, 3.34 mmol), $Pd_2(dba)_3$ (127 mg, 0.139 mmol), *rac*-BINAP (260 mg, 0.417 mmol), and cesium carbonate (1.27 g, 3.89 mmol). The vial was sealed with a Teflon-lined septum and flushed with argon for 5 minutes. Degassed toluene (14 mL) was added, and the resulting mixture was heated at 120 °C for 48 hours. Upon the completion of the reaction as judged by TLC analysis, the mixture was allowed to cool to room temperature, filtered through a Celite pad, and concentrated to a crude material which was purified by CombiFlash system (40g silica column, 5 minutes hexanes → 30 minutes 0-30% EtOAc/hexanes) to afford the title compound as a light yellow amorphous solid (1.40 g, quantitative yield). ^{1}H NMR (400 MHz, $CDCl_3$): δ 7.13 (td, J = 7.8, 4.2 Hz, 1H), 6.98 - 6.65 (m, 2H), 5.03 (dd, J = 6.1, 3.5 Hz, 0.5H), 4.80 - 4.55 (m, 1.5H), 4.42 (dd, J = 34.5, 16.1 Hz, 1H), 3.75 - 3.39 (m, 7H), 3.15 (ddd, J = 52.9, 15.5, 5.9 Hz, 1H), 2.98 - 2.60 (m, 5H), 1.62 - 1.27 (m, 18H). HRMS (*m/z*): calculated for $[C_{25}H_{37}N_3O_6 + H]^+$: 476.27606, found: 476.27542.

tert-Butyl 5-(4-(tert-butoxycarbonyl)piperazin-1-yl)-3-formyl-3,4-dihydroisoquinoline-2(1H)-carboxylate (9). To a 100-mL round-bottom flask containing a stir bar was charged with ester **8** (500 mg, 1.05 mmol) and anhydrous toluene (13 mL). Diisobutylaluminum hydride (1 M solution in toluene) (5.25 mL, 5.25 mmol) was added dropwise at -78 °C. After 2 h at -78 °C, reaction was quenched carefully with methanol then allowed to warm to 0 °C. A saturated solution of Rochelle salt was added, and the mixture was stirred at room temperature for an hour. The biphasic mixture was transferred to a separatory funnel. The aqueous layer was separated and extracted twice with ethyl acetate. The combined organic extract was dried over anhydrous sodium sulfate and concentrated under reduced pressure to afford the title compound as a crude material, which was used for the next step without purification. ^{1}H NMR (400 MHz, $CDCl_3$): δ

9.54 - 9.21 (m, 1H), 7.12 (td, J = 7.6, 5.1 Hz, 1H), 6.95 - 6.69 (m, 2H), 4.91 - 4.17 (m, 3H), 3.90 - 3.09 (m, 5H), 3.09 - 2.50 (m, 5H), 1.64 - 1.26 (m, 18H).

(R)-tert-Butyl 5-(4-(tert-butoxycarbonyl)piperazin-1-yl)-3-((methyl((S)-5,6,7,8-tetrahydroquinolin-8-yl)amino)methyl)-3,4-dihydroisoquinoline-2(1H)-carboxylate (11a) and **(S)-tert-Butyl 5-(4-(tert-butoxycarbonyl)piperazin-1-yl)-3-((methyl((S)-5,6,7,8-tetrahydroquinolin-8-yl)amino)methyl)-3,4-dihydroisoquinoline-2(1H)-carboxylate (11b)**. To a 20-mL scintillation vial equipped with magnetic stir bar was charged with amine **10** (114 mg, 0.705 mmol), sodium triacetoxyborohydride (179 mg, 0.846 mmol), and 1,2-dichloroethane (1.35 mL). After stirring for 5 minutes, a solution of aldehyde **9** (209 mg, 0.470 mmol) in 1,2-dichloroethane (1 mL) was added dropwise. The resulting mixture was stirred at room temperature for 48 hours. Upon the completion of the reaction as judged by TLC and LCMS, the mixture was quenched by the addition of 1N NaOH. The biphasic mixture was transferred to a separatory funnel. The aqueous layer was separated and extracted with DCM (3 times). The combined organic extract was dried over anhydrous sodium sulfate and concentrated under reduced pressure to a crude diastereomeric mixture (1:1 *d.r.*) which was separated and purified by CombiFlash system (24g GOLD silica column, 5 minutes DCM → 30 minutes 0-10% MeOH/DCM) to afford title compounds as yellow foamy solid. Compound **11a** (147 mg, 53 % yield). Upper R_f. ^{1}H NMR (400 MHz, $CDCl_3$): δ 8.23 (d, J = 4.7 Hz, 1H), 7.29 (d, J = 7.8 Hz, 1H), 7.05 (t, J = 7.7 Hz, 1H), 6.96 (dd, J = 7.7, 4.6 Hz, 1H), 6.79 (d, J = 7.9 Hz, 1H), 6.66 (dd, J = 14.9, 7.5 Hz, 1H), 4.66 - 4.37 (m, 2H), 3.85 (d, J = 17.0 Hz, 1H), 3.68 - 3.35 (m, 5H), 3.21 (d, J = 16.0 Hz, 1H), 2.92 (dt, J = 10.4, 4.5 Hz, 2H), 2.83 - 2.53 (m, 7H), 2.24 (s, 3H), 1.99 - 1.90 (m, 1H), 1.84 (q, J = 6.2 Hz, 2H), 1.47 (d, J = 2.7 Hz, 19H). HRMS (*m/z*): calculated for $[C_{34}H_{49}N_5O_4 + H]^+$: 592.38628, found: 592.38611. Compound **11b** (86 mg, 31 % yield). Lower

R_f. ^{1}H NMR (400 MHz, $CDCl_3$): δ 8.44 - 8.29 (m, 1H), 7.26 - 7.17 (m, 1H), 7.09 (q, J = 6.3, 4.8 Hz, 1H), 7.01 - 6.90 (m, 1H), 6.77 (dd, J = 20.4, 7.7 Hz, 2H), 4.51 (dd, J = 67.8, 12.3 Hz, 2H), 4.24 (d, J = 16.8 Hz, 1H), 3.71 - 3.19 (m, 6H), 2.93 (t, J = 9.0 Hz, 2H), 2.68 - 2.53 (m, 5H), 2.46 (dd, J = 12.8, 5.4 Hz, 1H), 2.33 (s, 3H), 1.86 (d, J = 8.5 Hz, 2H), 1.56 (d, J = 52.6 Hz, 21H). HRMS (*m/z*): calculated for $[C_{34}H_{49}N_5O_4 + H]^+$: 592.38628, found: 592.38507.

General procedure A: Global Boc Deprotection. To a 20-mL scintillation vial equipped with a magnetic stir bar was charged with the Boc-protected substrate (1 equiv) and DCM (0.13 M). Trifluoroacetic acid (36 equiv) was added dropwise, and the resulting mixture was stirred at room temperature overnight. Upon the completion of the reaction as judged by LCMS, the mixture was diluted with DCM, cooled in an ice-bath, and quenched by the addition of 3N NaOH until pH>12. The biphasic mixture was transferred to a separatory funnel. The aqueous layer was separated and extracted with DCM (3 times). The combined organic extract was dried over anhydrous sodium sulfate and concentrated under reduced pressure to a crude material which was purified by CombiFlash system using a gradient of solvent A (DCM) to solvent B (8:2:0.6 DCM/MeOH/NH_3 solution, 7N in MeOH) as eluent on a silica gel column to afford the final compound.

(S)-N-Methyl-N-(((R)-5-(piperazin-1-yl)-1,2,3,4-tetrahydroisoquinolin-3-yl)methyl)-5,6,7,8-tetrahydroquinolin-8-amine (**12a**). Following general procedure A. Boc-protected substrate **11a** (100 mg, 0.168 mmol), TFA (0.5 mL), and DCM (1.3 mL). The crude material was purified by CombiFlash (12g silica column, 5 minutes A → 30 minutes 0-100% B) to afford the title compound as a light yellow foam (67.5 mg, quantitative yield). ^{1}H NMR (400 MHz, $CDCl_3$): δ 8.43 (d, J = 4.7 Hz, 1H), 7.36 (d, J = 7.6 Hz, 1H), 7.17 - 7.01 (m, 2H), 6.88 (d, J = 7.8 Hz, 1H), 6.77 (d, J = 7.5 Hz, 1H), 4.66 (s, 2H), 4.22 - 4.11 (m, 1H), 4.08 - 3.95 (m, 2H), 3.05 - 2.87 (m,

8H), 2.86 - 2.56 (m, 6H), 2.44 (s, 4H), 2.11 - 1.87 (m, 3H), 1.80 - 1.64 (m, 1H). ^{13}C NMR (101 MHz, $CDCl_3$): δ 157.9, 151.6, 146.7, 136.9, 135.4, 134.0, 129.5, 126.3, 121.7, 121.7, 117.1, 64.5, 59.6, 52.9, 51.8, 47.8, 46.4, 40.5, 29.7, 29.2, 25.7, 21.3. HRMS (*m/z*): calculated for $[C_{24}H_{33}N_5 + H]^+$: 392.28142, found: 392.28082.

(S)-N-Methyl-N-(((S)-5-(piperazin-1-yl)-1,2,3,4-tetrahydroisoquinolin-3-yl)methyl)-5,6,7,8-tetrahydroquinolin-8-amine (**12b**). Following general procedure A. Boc-protected substrate **11b** (59.3 mg, 0.10 mmol), TFA (0.3 mL), and DCM (0.8 mL). The crude material was purified by CombiFlash (12g silica column, 5 minutes A → 30 minutes 0-100% B) to afford the title compound as a light yellow foam (32.7 mg, 83 % yield). ^{1}H NMR (400 MHz, $CDCl_3$): δ 8.44 (dd, J = 4.7, 2.0 Hz, 1H), 7.35 (dd, J = 7.7, 1.7 Hz, 1H), 7.15 - 7.02 (m, 2H), 6.94 - 6.85 (m, 1H), 6.85 - 6.75 (m, 1H), 6.58 (s, 1H), 4.23 (t, J = 6.4 Hz, 2H), 3.86 (dd, J = 9.9, 5.5 Hz, 1H), 3.37 - 3.17 (m, 1H), 3.07 - 2.86 (m, 5H), 2.69 (ddd, J = 41.9, 20.3, 10.7 Hz, 7H), 2.49 (s, 3H), 2.24 - 2.09 (m, 1H), 2.09 - 1.92 (m, 1H), 1.87 - 1.59 (m, 2H), 1.23 (s, 2H). ^{13}C NMR (101 MHz, $CDCl_3$): δ 157.0, 151.4, 151.3, 147.2, 137.2, 134.3, 126.7, 122.1, 121.9, 121.5, 117.6, 117.5, 77.4, 77.3, 77.1, 76.7, 52.3, 52.0, 51.8, 51.6, 45.9, 39.4, 36.8, 29.7, 29.0, 22.6, 21.4. HRMS (*m/z*): calculated for $[C_{24}H_{33}N_5 + H]^+$: 392.28142, found: 392.28090.

2-(tert-Butyl) 3-methyl (R)-5-(4-(tert-butoxycarbonyl)piperazin-1-yl)-3,4-dihydroisoquinoline-2,3(1H)-dicarboxylate (**14**). Compound **14** was prepared from ester **13** (107 mg, 0.289 mmol) according to the procedure described for the synthesis of **8**. Light yellow amorphous solid (122 mg, 89 % yield). ^{1}H NMR (400 MHz, $CDCl_3$): δ 7.13 (td, J = 7.8, 4.2 Hz, 1H), 6.98 - 6.65 (m, 2H), 5.03 (dd, J = 6.1, 3.5 Hz, 0.5H), 4.80 - 4.55 (m, 1.5H), 4.42 (dd, J = 34.5, 16.1 Hz, 1H), 3.75 - 3.39 (m, 7H), 3.15 (ddd, J = 52.9, 15.5, 5.9 Hz, 1H), 2.98 - 2.60 (m, 5H), 1.62 - 1.27 (m, 18H). HRMS (*m/z*): calculated for $[C_{25}H_{37}N_3O_6 + H]^+$, 476.27606; found,

476.27542. Normal phase chiral HPLC: 10% IPA/hexanes isocratic; 40 min; 1.0 mL/min; t_1 = 8.894 min; t_2 = 10.346 min; *e.r.* = 93:7.

tert-Butyl (R)-5-(4-(tert-butoxycarbonyl)piperazin-1-yl)-3-formyl-3,4-dihydroisoquinoline-2(1H)-carboxylate (**15**). Compound **15** was prepared from ester **14** (500 mg, 1.05 mmol) according to the procedure described for the synthesis of **9**. The crude material was used for the next step without purification ^{1}H NMR (400 MHz, $CDCl_3$): δ 9.54 - 9.21 (m, 1H), 7.12 (td, J = 7.6, 5.1 Hz, 1H), 6.95 - 6.69 (m, 2H), 4.91 - 4.17 (m, 3H), 3.90 - 3.09 (m, 5H), 3.09 - 2.50 (m, 5H), 1.64 - 1.26 (m, 18H).

tert-Butyl (R)-5-(4-(tert-butoxycarbonyl)piperazin-1-yl)-3-((((S)-5,6,7,8-tetrahydroquinolin-8-yl)amino)methyl)-3,4-dihydroisoquinoline-2(1H)-carboxylate (**17**). To a 250-mL round-bottom flask equipped with a magnetic stir bar was charged with amine **16** (2.37 g, 16.0 mmol), sodium triacetoxyborohydride (4.07 g, 19.2 mmol), and 1,2-dichloroethane (43 mL). After stirring for 5 minutes, a solution of aldehyde **15** (4.75 g, 10.7 mmol) in 1,2-dichloroethane (10 mL) was added dropwise. The resulting mixture was stirred at room temperature for 48 hours. Upon the completion of the reaction as judged by TLC and LCMS, the mixture was quenched by the addition of 1N NaOH. The biphasic mixture was transferred to a separatory funnel. The aqueous layer was separated and extracted with DCM (5 times). The combined organic extract was dried over anhydrous sodium sulfate and concentrated under reduced pressure to a crude material which was purified by CombiFlash system (120g silica column, 5 minutes DCM → 30 minutes 0-5% MeOH/DCM) to afford the title compound as a yellow amorphous solid (3.04 g, 49 % yield). ^{1}H NMR (400 MHz, $CDCl_3$): δ 8.36 - 8.29 (m, 1H), 7.35 (d, J = 7.5 Hz, 1H), 7.16 (t, J = 7.8 Hz, 1H), 7.09 - 7.01 (m, 1H), 6.93 - 6.79 (m, 2H), 4.67 (d, J = 16.8 Hz, 2H), 4.32 (d, J = 16.5 Hz, 1H), 3.86 - 3.22 (m, 6H), 2.95 (s, 2H), 2.85 - 2.61

(m, 6H), 2.59 - 2.24 (m, 2H), 1.95 (s, 2H), 1.65 (d, J = 8.7 Hz, 2H), 1.49 (d, J = 8.8 Hz, 18H). *d.r.* = 12:1 (determined by ^{1}H NMR of the purified product). HRMS (*m/z*): calculated for $[C_{33}H_{47}N_5O_4 + H]^+$, 578.37063; found: 578.36923.

General Procedure B for Side Chain Modifications via Reductive Amination: To a 20-mL scintillation vial equipped with a magnetic stir bar was charged with amine **17** (1 equiv), sodium triacetoxyborohydride (STAB-H) (1.8 equiv), and 1,2-dichloroethane (0.1 M). After stirring for 5 minutes, aldehyde or ketone (3 equiv) was added in one portion. The resulting mixture was stirred at room temperature for 48-72 hours. Additional equivalents of aldehyde/ketone might be added to drive the reaction to completion. Upon the completion of the reaction as judged by TLC and LCMS, the mixture was quenched with 1N NaOH. The biphasic mixture was transferred to a separatory funnel. The aqueous layer was separated and extracted with DCM 3 times. The combined organic extract was dried over anhydrous sodium sulfate and concentrated under reduced pressure to a crude material which was purified by CombiFlash system using a gradient of solvent A (DCM) to solvent B (MeOH) as eluent on a RediSep R_f GOLD silica column to afford the Boc-protected product.

General Procedure C for Side Chain Modifications via N-alkylation: To a 20-mL scintillation vial equipped with a magnetic stir bar was charged with amine **17** (1 equiv), DIPEA (3 equiv), and 1,2-dichloroethane (0.1 M). Alkyl bromide (3 equiv) was added in one portion, and the resulting mixture was heated at 70 °C overnight. Upon the completion of the reaction as judged by TLC and LCMS, the mixture was quenched with a solution of saturated $NaHCO_3$. The biphasic mixture was transferred to a separatory funnel. The aqueous layer was separated and extracted with DCM 3 times. The combined organic extract was dried over anhydrous sodium sulfate and concentrated under reduced pressure to a crude material which was purified by

CombiFlash system using a gradient of solvent A (DCM) to solvent B (MeOH) as eluent on a RediSep R_f GOLD silica column to afford the Boc-protected product.

(S)-N-Ethyl-N-(((R)-5-(piperazin-1-yl)-1,2,3,4-tetrahydroisoquinolin-3-yl)methyl)-5,6,7,8-tetrahydroquinolin-8-amine (**19a**). Compound **19a** was synthesized by a two-step sequence. Step 1 (general procedure B): Amine **17** (150 mg, 0.260 mmol), STAB-H (99 mg, 0.467 mmol), DCE (2.60 mL), and acetaldehyde (45 μL, 0.780 mmol). Purification by CombiFlash (12g GOLD silica column, 5 minutes DCM → 30 min 0-10% MeOH/DCM) provided Boc-protected intermediate **18a** as a yellow foamy solid (87.4 mg, 56 % yield). ^{1}H NMR (400 MHz, $CDCl_3$): δ 8.29 (d, J = 5.5 Hz, 1H), 7.28 (d, J = 7.6 Hz, 1H), 7.09 (t, J = 7.8 Hz, 1H), 6.97 (dd, J = 7.7, 4.6 Hz, 1H), 6.82 (d, J = 7.9 Hz, 1H), 6.79 - 6.67 (m, 1H), 4.61 (d, J = 17.5 Hz, 2H), 4.06 (d, J = 16.9 Hz, 1H), 3.79 - 3.30 (m, 6H), 2.98 (s, 2H), 2.76 - 2.57 (m, 7H), 2.38 (dd, J = 13.8, 7.0 Hz, 1H), 2.05 (s, 1H), 1.94 (s, 1H), 1.75 (dd, J = 17.2, 6.8 Hz, 1H), 1.48 (s, 20H), 0.92 (t, J = 7.0 Hz, 3H). HRMS calculated for $[C_{35}H_{51}N_5O_4 + H]^+$: 606.40193, found: 606.40175. Step 2 (general procedure A): Compound **18a** (87.4 mg, 0.144 mmol), TFA (0.4 mL, 5.19 mmol), and DCM (1 mL). The crude material was purified by CombiFlash (12g silica column, 5 minutes A → 30 minutes 0-60% B) to afford the title compound as a light yellow foam (47.9 mg, 82 % yield). ^{1}H NMR (400 MHz, $CDCl_3$): δ 8.43 (dd, J = 4.7, 1.7 Hz, 1H), 7.30 (dd, J = 7.7, 1.7 Hz, 1H), 7.12 - 6.97 (m, 2H), 6.84 (d, J = 7.8 Hz, 1H), 6.74 (d, J = 7.6 Hz, 1H), 4.14 - 4.03 (m, 2H), 3.88 (d, J = 15.2 Hz, 1H), 3.09 - 2.61 (m, 17H), 2.46 (dd, J = 13.2, 10.4 Hz, 1H), 2.17 (dd, J = 16.5, 10.8 Hz, 1H), 2.06 - 1.85 (m, 3H), 1.76 - 1.64 (m, 1H), 1.09 (t, J = 7.1 Hz, 3H). ^{13}C NMR (101 MHz, $CDCl_3$): δ 159.0, 151.8, 146.7, 136.6, 136.3, 134.0, 130.0, 126.1, 121.8, 121.4, 116.9, 61.4, 57.3, 53.2, 52.4, 48.6, 48.1, 46.7, 30.0, 29.5, 29.0, 21.9, 15.2. HRMS (*m/z*): calculated for $[C_{25}H_{35}N_5 + H]^+$: 406.29707, found: 406.29618.

(S)-N-(((R)-5-(Piperazin-1-yl)-1,2,3,4-tetrahydroisoquinolin-3-yl)methyl)-N-propyl-5,6,7,8-tetrahydroquinolin-8-amine (**19b**). Compound **19b** was synthesized by a two-step sequence (general procedure B → general procedure A). White foam (65 % yield over 2 steps). ^{1}H NMR (400 MHz, $CDCl_3$): δ 8.43 (dd, J = 4.8, 1.7 Hz, 1H), 7.31 (dd, J = 7.7, 1.7 Hz, 1H), 7.13 - 6.98 (m, 2H), 6.85 (ddd, J = 7.9, 3.8, 1.1 Hz, 1H), 6.80 - 6.69 (m, 1H), 4.17 - 4.01 (m, 2H), 3.94 (d, J = 15.2 Hz, 1H), 3.15 - 2.33 (m, 18H), 2.20 - 2.02 (m, 2H), 2.00 - 1.85 (m, 2H), 1.76 - 1.65 (m, 1H), 1.56 - 1.41 (m, 2H), 0.87 (t, J = 7.3 Hz, 3H). ^{13}C NMR (101 MHz, $CDCl_3$): δ 159.1, 151.8, 151.6, 146.7, 136.6, 134.0, 130.1, 126.1, 121.8, 121.4, 116.8, 61.6, 57.9, 56.5, 53.3, 52.5, 52.2, 51.7, 48.8, 46.7, 30.0, 29.8, 29.5, 23.1, 22.1, 11.9. HRMS (*m/z*): calculated for $[C_{26}H_{37}N_5 + H]^+$: 420.31272, found: 420.31223.

(S)-N-(Cyclopropylmethyl)-N-(((R)-5-(piperazin-1-yl)-1,2,3,4-tetrahydroisoquinolin-3-yl)methyl)-5,6,7,8-tetrahydroquinolin-8-amine (**19c**). Compound **19c** was synthesized by a two-step sequence (general procedure B → general procedure A). White foam (77 % yield over 2 steps). ^{1}H NMR (400 MHz, $CDCl_3$): δ 8.48 (dd, J = 4.7, 1.7 Hz, 1H), 7.36 (dd, J = 7.7, 1.7 Hz, 1H), 7.19 - 7.02 (m, 2H), 6.91 (dd, J = 7.9, 4.1 Hz, 1H), 6.81 (dd, J = 7.7, 4.1 Hz, 1H), 4.28 (dd, J = 10.3, 6.2 Hz, 1H), 4.18 (d, J = 15.2 Hz, 1H), 3.97 (d, J = 15.2 Hz, 1H), 3.58 - 2.56 (m, 18H), 2.32 - 2.11 (m, 2H), 2.07 - 1.91 (m, 2H), 1.84 - 1.71 (m, 1H), 1.04 - 0.93 (m, 1H), 0.53 (dqt, J = 26.1, 8.8, 4.3 Hz, 2H), 0.28 - 0.01 (m, 2H). ^{13}C NMR (101 MHz, $CDCl_3$): δ 159.0, 151.7, 151.5, 146.6, 136.4, 133.8, 130.0, 125.9, 121.7, 121.2, 116.7, 61.6, 59.2, 57.5, 53.1, 52.4, 52.1, 51.6, 48.7, 46.6, 29.9, 29.4, 29.3, 22.0, 11.3, 4.6, 3.5. HRMS (*m/z*): calculated for $[C_{27}H_{37}N_5 + H]^+$: 432.31272, found: 432.31179.

(S)-N-Isopropyl-N-(((R)-5-(piperazin-1-yl)-1,2,3,4-tetrahydroisoquinolin-3-yl)methyl)-5,6,7,8-tetrahydroquinolin-8-amine (**19d**). Compound **19d** was synthesized by a two-step

sequence (general procedure B → general procedure A). White foam (47 % yield over 2 steps). ^{1}H NMR (400 MHz, $CDCl_3$): δ 8.41 (dd, J = 4.7, 1.7 Hz, 1H), 7.25 (dd, J = 9.5, 1.9 Hz, 1H), 7.08 - 6.95 (m, 2H), 6.82 (d, J = 7.7 Hz, 1H), 6.68 (d, J = 7.6 Hz, 1H), 4.12 - 3.97 (m, 2H), 3.43 (d, J = 15.3 Hz, 1H), 3.24 - 3.07 (m, 2H), 3.07 - 2.49 (m, 13H), 2.26 (d, J = 10.9 Hz, 2H), 2.05 - 1.94 (m, 3H), 1.74 (dt, J = 11.2, 5.6 Hz, 1H), 1.11 (dd, J = 27.8, 6.6 Hz, 6H). ^{13}C NMR (101 MHz, $CDCl_3$): δ 159.4, 151.7, 151.5, 146.7, 136.7, 133.5, 129.6, 126.1, 121.7, 121.4, 116.9, 60.7, 53.5, 53.2, 52.9, 52.1, 47.8, 46.6, 29.4, 28.7, 22.0, 22.0, 21.4. HRMS (*m/z*): calculated for $[C_{26}H_{37}N_5 + H]^+$: 420.31272, found: 420.31198.

(S)-N-(Cyclohexylmethyl)-N-(((R)-5-(piperazin-1-yl)-1,2,3,4-tetrahydroisoquinolin-3-yl)methyl)-5,6,7,8-tetrahydroquinolin-8-amine (**19e**). Compound **19e** was synthesized by a two-step sequence (general procedure B → general procedure A). White foam (29 % yield over 2 steps). ^{1}H NMR (400 MHz, $CDCl_3$): δ 8.42 (dd, J = 4.7, 1.7 Hz, 1H), 7.30 (dd, J = 7.7, 1.7 Hz, 1H), 7.13 - 6.96 (m, 2H), 6.84 (dt, J = 8.0, 1.9 Hz, 1H), 6.80 - 6.68 (m, 1H), 4.12 (d, J = 15.1 Hz, 1H), 4.08 - 3.96 (m, 2H), 3.11 (dd, J = 12.8, 5.3 Hz, 1H), 3.00 - 2.59 (m, 14H), 2.39 - 2.28 (m, 2H), 2.10 (dd, J = 16.0, 11.1 Hz, 2H), 1.99 - 1.58 (m, 9H), 1.45 - 1.37 (m, 1H), 1.25 - 1.09 (m, 3H), 0.86 - 0.74 (m, 2H). ^{13}C NMR (101 MHz, $CDCl_3$): δ 159.3, 151.9, 151.6, 146.6, 136.4, 134.0, 130.3, 126.1, 121.8, 121.3, 116.8, 62.0, 58.3, 53.2, 52.6, 49.0, 46.7, 37.9, 31.9, 31.7, 30.7, 30.0, 29.5, 27.0, 26.4, 26.3, 22.3. HRMS (*m/z*): calculated for $[C_{30}H_{43}N_5 + H]^+$: 474.35967, found: 474.35953.

(S)-N-((4,4-Difluorocyclohexyl)methyl)-N-(((R)-5-(piperazin-1-yl)-1,2,3,4-tetrahydroisoquinolin-3-yl)methyl)-5,6,7,8-tetrahydroquinolin-8-amine (**19f**). Compound **19f** was synthesized by a two-step sequence (general procedure B → general procedure A). White foam (72 % yield over 2 steps). ^{1}H NMR (400 MHz, $CDCl_3$): δ 8.43 (dd, J = 4.8, 1.7 Hz,

1H), 7.38 - 7.31 (m, 1H), 7.14 - 7.04 (m, 2H), 6.88 (dd, J = 7.9, 1.1 Hz, 1H), 6.79 (dd, J = 7.6, 1.1 Hz, 1H), 4.23 - 3.96 (m, 3H), 3.12 - 2.85 (m, 9H), 2.84 - 2.60 (m, 6H), 2.37 (dd, J = 13.5, 8.5 Hz, 1H), 2.16 - 1.79 (m, 9H), 1.52 (s, 5H), 1.16 (t, J = 12.1 Hz, 2H). ^{13}C NMR (101 MHz, $CDCl_3$): δ 158.6, 151.7, 146.5, 136.3, 136.3, 133.7, 129.9, 125.9, 121.6, 121.3, 116.7, 61.6, 60.3, 58.4, 53.1, 52.4, 48.9, 46.5, 35.7, 33.6, 33.5, 33.4, 33.3, 33.1, 33.0, 30.1, 30.0, 29.3, 27.3, 27.2, 27.2, 27.1, 22.1. ^{19}F NMR (376 MHz, $CDCl_3$, TFA standard): δ -15.42 (d, J = 235.6 Hz), -25.64 (d, J = 232.3 Hz). HRMS (*m/z*): calculated for $[C_{30}H_{41}F_2N_5 + H]^+$: 510.34083, found: 510.34065.

2-((((R)-5-(Piperazin-1-yl)-1,2,3,4-tetrahydroisoquinolin-3-yl)methyl)((S)-5,6,7,8-tetrahydroquinolin-8-yl)amino)ethan-1-ol (**19g**). Compound **19g** was synthesized by a two-step sequence (general procedure C → general procedure A). White foam (78 % yield over 2 steps). ^{1}H NMR (400 MHz, $CDCl_3$): δ 8.43 (dd, J = 4.8, 1.7 Hz, 1H), 7.36 (dt, J = 7.7, 1.3 Hz, 1H), 7.11 - 7.06 (m, 2H), 6.86 (dd, J = 7.9, 1.2 Hz, 1H), 6.74 (dd, J = 7.6, 1.1 Hz, 1H), 4.14 - 4.04 (m, 2H), 3.79 (d, J = 15.5 Hz, 1H), 3.70 - 3.41 (m, 4H), 3.16 - 3.11 (m, 1H), 3.09 - 2.54 (m, 16H), 2.27 - 2.15 (m, 2H), 2.03 (dtt, J = 12.8, 5.1, 2.7 Hz, 1H), 1.98 - 1.85 (m, 1H), 1.82 - 1.68 (m, 1H). ^{13}C NMR (101 MHz, $CDCl_3$): δ 158.2, 151.6, 146.4, 137.1, 136.4, 133.8, 129.6, 126.0, 121.7, 121.5, 116.7, 63.0, 60.1, 56.9, 55.7, 53.0, 52.5, 48.5, 46.4, 29.8, 29.1, 26.4, 21.9. HRMS (*m/z*): calculated for $[C_{25}H_{35}N_5O + H]^+$: 422.29199, found: 422.29351.

(S)-N-(2-Methoxyethyl)-N-(((R)-5-(piperazin-1-yl)-1,2,3,4-tetrahydroisoquinolin-3-yl)methyl)-5,6,7,8-tetrahydroquinolin-8-amine (**19h**). Compound **19h** was synthesized by a two-step sequence (general procedure B → general procedure A). Yellow foam (69 % yield over 2 steps). ^{1}H NMR (400 MHz, $CDCl_3$): δ 8.38 (dd, J = 4.8, 1.7 Hz, 1H), 7.31 (dt, J = 7.7, 1.4 Hz, 1H), 7.14 - 6.97 (m, 2H), 6.86 (td, J = 7.9, 1.2 Hz, 1H), 6.82 - 6.71 (m, 1H), 5.46 (s, broad, 2H), 4.25 (dd, J = 15.3, 4.5 Hz, 1H), 4.12 (dd, J = 10.3, 6.5 Hz, 1H), 4.02 (dd, J = 15.4, 4.1 Hz, 1H),

3.41 - 3.29 (m, 2H), 3.27 (s, 3H), 3.19 (dt, J = 13.7, 4.7 Hz, 2H), 2.92 (dddd, J = 24.5, 19.3, 11.9, 5.1 Hz, 7H), 2.81 - 2.41 (m, 8H), 2.14 - 2.01 (m, 1H), 2.01 - 1.82 (m, 2H), 1.69 (dtt, J = 11.4, 8.9, 4.8 Hz, 1H). ^{13}C NMR (101 MHz, $CDCl_3$): δ 158.4, 151.6, 146.5, 136.9, 134.1, 129.1, 126.5, 121.7, 121.7, 121.4, 117.4, 72.4, 62.7, 58.8, 57.1, 53.0, 52.7, 52.1, 51.7, 46.9, 46.2, 29.2, 28.1, 22.0. HRMS (*m/z*): calculated for $[C_{26}H_{37}N_5O + H]^+$: 436.30764, found: 436.30781.

(R)-N-Methyl-1-(3-methylpyridin-2-yl)-N-((5-(piperazin-1-yl)-1,2,3,4-tetrahydroisoquinolin-3-yl)methyl)methanamine (**21a**). Compound **21a** was prepared according to the procedure described for the synthesis of **21b**. Orange semi solid (59 % yield over two steps). ^{1}H NMR (500 MHz, $CDCl_3$): δ 8.35 (d, *J*= 4.7 Hz, 1H), 7.43 (d, *J*= 7.5 Hz, 1H), 7.09-7.06 (m, 2H), 6.84 (d, *J*= 7.5 Hz, 1H), 6.73 (d, *J*= 7.5 Hz, 1H), 4.03 (d, *J*= 15.0 Hz, 1H), 4.00 (d, *J*= 15.0 Hz, 1H), 3.73 (d, *J*= 12.5 Hz, 1H), 3.62 (d, *J*= 12.5 Hz, 1H), 3.02-2.88 (m, 8H), 2.66 (t, *J*= 7.2 Hz, 3H), 2.61 (dd, *J= 12.0, 9.5* Hz, 1H), 2.52 (dd, *J= 12.2, 3.5* Hz, 1H), 2.44 (s, 3H), 2.28 (s, 3H), 2.18 (dd, *J= 17.0, 11.0* Hz, 1H). ^{13}C NMR (125 MHz, $CDCl_3$): δ 156.8, 151.8, 146.2, 138.1, 136.4, 133.0, 129.8, 126.1, 122.5, 121.6, 116.8, 63.7, 63.6, 53.2, 51.3, 48.7, 46.6, 43.0, 30.3, 18.5. HRMS (*m/z*): calculated for $[C_{22}H_{32}N_5 + H]^+$: 366.26522, found 366.26504.

(R)-1-(3,5-Dimethylpyridin-2-yl)-N-methyl-N-((5-(piperazin-1-yl)-1,2,3,4-tetrahydroisoquinolin-3-yl)methyl)methanamine (**21b**). To a 20-mL scintillation vial was added aldehyde **15** (270 mg, 0.605 mmol), amine **S2** (100 mg, 0.666 mmol), DCE (3.0 mL), and sodium triacetoxyborohydride (192 mg, 0.908 mmol) then the mixture was allowed to stir at room temperature overnight. The reaction was diluted with DCM, washed with 1N NaOH, dried over Na_2SO_4, filtered, and concentrated to afford a crude material which was purified via CombiFlash (2 minutes DCM → 5 minutes at 10% B (80:20:3, DCM:MeOH:NH_4OH) → 9 minutes at 50% B). The fractions were concentrated to afford a yellow oil which was dissolved

in DCM (5 mL) and TFA (0.5 mL). The reaction was allowed to stir at room temperature overnight. The reaction was diluted with DCM, washed with 1N NaOH, dried over Na_2SO_4, filtered, and concentrated to afford a crude material which was purified via CombiFlash (2 minutes DCM → 5 minutes at 10% B (80:20:3, DCM:MeOH:NH_4OH) → 9 minutes 50% B) to afford the title compound as an orange semi solid (110 mg, 48% yield over two steps). ^{1}H NMR (500 MHz, $CDCl_3$): δ 8.19 (s, 1H), 7.09 (t, *J*= 7.7 Hz, 1H), 6.87 (d, *J*= 7.8 Hz, 1H), 6.75 (d, *J*= 7.5 Hz, 1H), 4.04 (s, 2H), 3.73 (d, *J*= 12.4 Hz, 1H), 3.60 (d, *J*= 12.4 Hz, 1H), 3.03-2.88 (m, 9H), 2.69-2.65 (m, 2H), 2.58 (dd, *J*= 12.3, 9.6 Hz, 1H), 2.51 (dd, *J*= 12.3, 3.4 Hz, 1H), 2.41 (s, 3H), 2.27 (3, 3H), 2.26 (s, 3H), 2.16 (dd, *J*= 16.8, 11.0 Hz, 1H). ^{13}C NMR (100 MHz, $CDCl_3$): δ 153.7, 151.7, 146.4, 138.9, 136.3, 132.2, 131.8, 129.8, 126.0, 121.6, 116.8, 63.4, 63.1, 53.1, 51.2, 48.6, 46.5, 42.9, 30.1, 18.3, 17.9. HRMS (*m/z*): calculated for $[C_{23}H_{34}N_5 + H]^+$: 380.28087, found 380.28068.

(R)-N-Methyl-1-(5-methylpyridin-2-yl)-N-((5-(piperazin-1-yl)-1,2,3,4-tetrahydroisoquinolin-3-yl)methyl)methanamine (**21c**). Compound **21c** was prepared according to the procedure described for the synthesis of **21b**. Orange semi solid (67 % yield over two steps). ^{1}H NMR (500 MHz, $CDCl_3$): *δ* 8.32 (d, *J*= 0.5 Hz, 1H), 7.42 (dd, *J*= 7.9, 1.6 Hz, 1H), 7.29 (d, *J*= 7.9 Hz, 1H), 7.05 (t, *J*= 7.6 Hz, 1H), 6.82 (d, *J*= 7.6 Hz, 1H), 6.72 (d, *J*= 7.6 Hz, 1H), 4.04 (d, *J*= 15.3 Hz, 1H), 4.01 (d, *J*= 15.3 Hz, 1H), 3.71 (d, *J*= 13.9 Hz, 1H), 3.57 (d, *J*= 13.9 Hz, 1H), 2.99-2.85 (m, 8H), 2.65 (brs, 2H), 2.56 (dd, *J= 12.6, 10.0* Hz, 1H), 2.47 (dd, *J= 12.6, 3.4* Hz, 1H), 2.34 (brs, 3H), 2.28 (s, 3H), 2.25 (s, 3H), 2.14 (dd, *J= 16.8, 11.3* Hz, 1H); ^{13}C NMR (125 MHz, $CDCl_3$): *δ* 156.3, 151.7, 149.4, 137.1, 136.5, 131.4, 129.8, 126.0, 122.6, 121.6, 116.8, 64.4, 63.2, 53.2, 51.3, 48.7, 46.5, 43.2, 30.2, 18.1. HRMS (*m/z*): calculated for $[C_{22}H_{32}N_5 + H]^+$: 366.26522, found 366.26501.

(S)-N,3-Dimethyl-N-(((R)-5-(piperazin-1-yl)-1,2,3,4-tetrahydroisoquinolin-3-yl)methyl)-5,6,7,8-tetrahydroquinolin-8-amine (**21d**). To a 20-mL scintillation vial was added amine **S4** (0.166 g, 0.943 mmol), DCM (5 mL), sodium triacetoxyborohydride (0.285 g, 1.35 mmol), and aldehyde **15** (0.400 g, 0.897 mmol). The reaction mixture was allowed to stir over night. The reaction was diluted with DCM, washed with 1M NaOH, dried with Na_2SO_4, filtered, and concentrated to afford a yellow oil. The crude material was purified via CombiFlash (2 minutes DCM → 5 minutes at 10% B (80:20:3, DCM:MeOH:NH_4OH) → 9 minutes at 50% B). The fractions were concentrated to afford a yellow oil which was dissolved in DCM (3 mL) and TFA (0.6 mL) then the mixture was allowed to stir over night. The reaction was diluted with DCM, washed with 1M NaOH, dried with Na_2SO_4, filtered and concentrated to afford a yellow oil. The crude material was purified via CombiFlash (2 minutes DCM → 5 minutes at 10% B (80:20:3, DCM:MeOH:NH_4OH) → 9 minutes at 50% B). The fractions were concentrated to afford the title compound as a yellow oil. (0.122 g, 0.301 mmol, 63 % yield over 2 steps). ^{1}H NMR (500 MHz, $CDCl_3$): δ 8.28 (d, *J*= 1.4 Hz, 1H), 7.14 (d, *J*= 1.0 Hz, 1H), 7.07 (t, *J*= 7.8 Hz, 1H), 6.85 (d, *J*= 7.6 Hz, 1H), 6.74 (d, *J*= 7.6 Hz, 1H), 4.04 (d, *J*= 15.2 Hz, 1H), 3.91 (d, *J*= 15.2 Hz, 1H), 3.91-3.88 (m, 1H), 3.01-2.91 (m, 6H), 2.85-2.60 (m, 6H), 2.55-2.47 (m, 1H), 2.51 (s, 3H), 2.26 (s, 3H), 2.14 (dd, *J*= 16.1, 10.6 Hz, 1H), 2.05-1.91 (m, 2H), 1.72-1.63 (m, 1H). ^{13}C NMR (125 MHz, $CDCl_3$): δ 155.1, 151.9, 147.4, 137.2, 136.8, 133.2, 130.8, 130.1, 126.0, 121.8, 116.8, 64.3, 59.9, 53.3, 51.7, 48.8, 46.7, 41.6, 30.3, 29.2, 26.3, 21.3, 18.1. HRMS (*m/z*): calculated for $[C_{25}H_{36}N_5 + H]^+$: 406.29652, found 406.29611.

tert-Butyl (R)-5-bromo-3-formyl-3,4-dihydroisoquinoline-2(1H)-carboxylate (**22**). Compound **22** was prepared according to the procedure described for the synthesis of **9** starting with ester **13** (10 g, 27.0 mmol), anhydrous toluene (270 mL), and DIBAL-H (1 M solution in

toluene) (80 mL, 80 mmol). The crude material was used for the next step without purification. ^{1}H NMR (400 MHz, $CDCl_3$): δ 9.52 (d, J = 5.5 Hz, 1H), 7.53 - 7.36 (m, 1H), 7.18 - 6.92 (m, 2H), 4.96 (dd, J = 7.3, 3.2 Hz, 0.5H), 4.72 (dd, J = 16.7, 6.8 Hz, 1H), 4.66 - 4.37 (m, 1.5H), 3.58 - 3.28 (m, 1H), 3.05 (ddd, J = 33.6, 16.6, 6.7 Hz, 1H), 1.49 (d, J = 22.7 Hz, 9H).

tert-Butyl (R)-5-bromo-3-((methyl((S)-5,6,7,8-tetrahydroquinolin-8-yl)amino)methyl)-3,4-dihydroisoquinoline-2(1H)-carboxylate (**23**). To a 500-mL round-bottom flask equipped with magnetic stir bar was charged with amine **10** (6.57 g, 40.5 mmol), sodium triacetoxyborohydride (10.3 g, 48.6 mmol), and 1,2-dichloroethane (100 mL). After stirring for 5 minutes, a solution of aldehyde **22** (9.19 g, 27.0 mmol) in 1,2-dichloroethane (35 mL) was added dropwise. The resulting mixture was stirred at room temperature for 48 hours. Upon the completion of the reaction as judged by TLC and LCMS, the mixture was quenched by addition of saturated $NaHCO_3$ solution. The biphasic mixture was transferred to a separatory funnel. The aqueous layer was separated and extracted with DCM (3 times). The combined organic extract was dried over anhydrous sodium sulfate and concentrated under reduced pressure to a crude material which was purified by CombiFlash system (220g GOLD silica column, 5 minutes DCM → 30 minutes 0-5% MeOH/DCM) to afford the title compound as a colorless amorphous solid (10.5 g, 80 % yield). ^{1}H NMR (400 MHz, $CDCl_3$): δ 8.30 (s, 1H), 7.35 (d, J = 7.8 Hz, 1H), 7.28 (s, 1H), 6.94 (t, J = 7.4 Hz, 2H), 6.87 (s, 1H), 4.83 - 4.30 (m, 2H), 3.96 - 3.60 (m, 2H), 3.14 (d, J = 17.0 Hz, 1H), 2.84 - 2.70 (m, 2H), 2.70 - 2.48 (m, 2H), 2.36 (s, 4H), 2.09 - 1.72 (m, 3H), 1.62 (s, 1H), 1.47 (s, 9H). HRMS (*m/z*): calculated for $[C_{25}H_{32}BrN_3O_2 + H]^+$: 486.17561, found: 486.17731.

General procedure D for Late-stage Buchwald-Hartwig Coupling: To an oven-dried Biotage 5-10 mL microwave vial equipped with a magnetic stir bar was charged with compound **23** (1 equiv), $Pd_2(dba)_3$ (0.05 equiv, 5 mol %), *rac*-BINAP (0.15 equiv, 15 mol %), cesium carbonate

(1.4 equiv), and amine (if solid) (1.2 equiv). The vial was sealed with a Teflon-lined septum and flushed with argon for 5 minutes. Degassed toluene (0.2 M) and amine (if liquid) (1.2 equiv) were added successively via a syringe, and the vessel was degassed with argon for 5 minutes. The resulting mixture was heated at 120 °C for 24 hours. Upon the completion of the reaction as judged by TLC and LCMS, the mixture was allowed to cool to room temperature, filtered through a Celite pad, and concentrated to a crude material which was purified by CombiFlash system using a gradient of solvent A (DCM) to solvent B (MeOH) as eluent on a RediSep Rf GOLD silica column to afford the Boc-protected product.

(S)-N-(((R)-5-((1R,4R)-2,5-Diazabicyclo[2.2.1]heptan-2-yl)-1,2,3,4-tetrahydroisoquinolin-3-yl)methyl)-N-methyl-5,6,7,8-tetrahydroquinolin-8-amine (**25a**). Compound **25a** was synthesized by a two-step sequence (general procedure D → general procedure A). Light yellow foam (71 % yield over two steps). ^{1}H NMR (400 MHz, $CDCl_3$): δ 8.37 (s, 1H), 7.38 (d, J = 7.7 Hz, 1H), 7.16 - 7.02 (m, 2H), 6.99 (d, J = 8.0 Hz, 1H), 6.73 (d, J = 7.6 Hz, 1H), 6.22 (s, 2H), 4.34 (dd, J = 16.0, 4.7 Hz, 1H), 4.21 - 3.96 (m, 4H), 3.79 - 3.70 (m, 1H), 3.50 - 3.38 (m, 1H), 3.27 - 2.54 (m, 9H), 2.27 (d, J = 2.9 Hz, 3H), 2.11 - 1.80 (m, 5H), 1.73 (d, J = 8.9 Hz, 1H). ^{13}C NMR (101 MHz, methanol-d_4): δ 157.4, 150.4, 147.5, 139.5, 136.6, 133.4, 128.1, 126.9, 123.6, 121.2, 117.4, 66.7, 60.2, 60.2, 59.6, 58.8, 52.9, 52.4, 46.6, 36.3, 35.9, 30.0, 29.7, 22.5, 22.3. HRMS (*m/z*): calculated for $[C_{25}H_{33}N_5 + H]^+$: 404.28142, found: 404.28088.

(S)-N-(((R)-5-((1S,4S)-2,5-Diazabicyclo[2.2.1]heptan-2-yl)-1,2,3,4-tetrahydroisoquinolin-3-yl)methyl)-N-methyl-5,6,7,8-tetrahydroquinolin-8-amine (**25b**). Compound **25b** was synthesized by a two-step sequence (general procedure D → general procedure A). Yellow foam (511 mg, 82 % yield). ^{1}H NMR (400 MHz, $CDCl_3$): δ 8.31 (dd, J = 4.7, 1.8 Hz, 1H), 7.20 (dd, J

= 7.7, 1.7 Hz, 1H), 6.95 - 6.83 (m, 2H), 6.41 (dd, J = 14.1, 7.8 Hz, 2H), 3.96 - 3.79 (m, 4H), 3.69 (dd, J = 9.0, 2.5 Hz, 1H), 3.57 (s, 1H), 3.35 - 3.30 (m, 1H), 2.92 (dd, J = 10.2, 2.1 Hz, 1H), 2.71 - 2.51 (m, 7H), 2.43 - 2.30 (m, 5H), 2.11 (dd, J = 15.8, 10.2 Hz, 1H), 1.96 - 1.78 (m, 4H), 1.58 (ddd, J = 9.7, 5.2, 2.8 Hz, 2H). ^{13}C NMR (101 MHz, $CDCl_3$): δ 157.6, 147.7, 146.5, 136.8, 136.3, 133.5, 125.2, 124.7, 121.2, 117.5, 112.5, 77.4, 64.1, 61.5, 59.6, 59.4, 56.8, 51.4, 48.7, 41.2, 36.5, 32.7, 29.0, 25.2, 21.0. HRMS (*m/z*): calculated for $[C_{25}H_{33}N_5 + H]^+$: 404.28142, found: 404.28069.

(S)-N-(((R)-5-(3,3-Dimethylpiperazin-1-yl)-1,2,3,4-tetrahydroisoquinolin-3-yl)methyl)-N-methyl-5,6,7,8-tetrahydroquinolin-8-amine (**25c**). Compound **25c** was synthesized by a two-step sequence (general procedure D → general procedure A). Yellow foam (51 % yield over two steps). ^{1}H NMR (400 MHz, $CDCl_3$): *δ* 8.38 (dd, J = 4.8, 1.7 Hz, 1H), 7.25 - 7.20 (m, 1H), 7.03 - 6.90 (m, 2H), 6.75 (d, J = 7.8 Hz, 1H), 6.67 (d, J = 7.6 Hz, 1H), 3.96 (d, J = 15.3 Hz, 1H), 3.89 - 3.76 (m, 2H), 3.00 - 2.30 (m, 17H), 2.12 (dd, J = 16.5, 10.4 Hz, 1H), 1.99 - 1.83 (m, 3H), 1.65 - 1.56 (m, 1H), 1.12 (d, J = 25.6 Hz, 6H). ^{13}C NMR (101 MHz, $CDCl_3$): *δ* 157.8, 151.6, 146.6, 136.5, 136.4, 133.5, 130.0, 125.8, 121.6, 121.3, 116.8, 77.4, 64.3, 63.5, 59.8, 53.2, 51.5, 50.0, 48.6, 41.8, 41.2, 30.1, 29.0, 25.9, 21.1. HRMS (*m/z*): calculated for $[C_{26}H_{37}N_5 + H]^+$: 420.31272, found: 420.31334.

(S)-N-(((R)-5-((3S,5R)-3,5-Dimethylpiperazin-1-yl)-1,2,3,4-tetrahydroisoquinolin-3-yl)methyl)-N-methyl-5,6,7,8-tetrahydroquinolin-8-amine (**25d**). Compound **25d** was synthesized by a two-step sequence (general procedure D → general procedure A). White foam (52 % yield over two steps). ^{1}H NMR (400 MHz, $CDCl_3$): *δ* 8.38 (dd, J = 4.7, 1.7 Hz, 1H), 7.29 - 7.19 (m, 1H), 7.02 - 6.90 (m, 2H), 6.75 (d, J = 7.9 Hz, 1H), 6.66 (d, J = 7.6 Hz, 1H), 3.97 (d, J = 15.2 Hz, 1H), 3.88 - 3.76 (m, 2H), 2.98 - 2.55 (m, 11H), 2.41 (d, J = 26.6 Hz, 5H), 2.19 - 2.02

(m, 2H), 1.91 (td, J = 15.0, 12.9, 7.9 Hz, 3H), 1.66 - 1.57 (m, 1H), 0.97 (dd, J = 22.7, 6.3 Hz, 6H). ^{13}C NMR (101 MHz, $CDCl_3$): δ 158.0, 151.2, 146.7, 136.5, 133.6, 129.9, 125.8, 121.5, 121.4, 116.8, 64.3, 59.8, 59.6, 58.5, 51.5, 51.0, 50.8, 48.6, 41.4, 30.1, 29.1, 26.1, 21.1, 19.7, 19.6. HRMS (*m/z*): calculated for $[C_{26}H_{37}N_5 + H]^+$: 420.31272, found: 420.31131.

(S)-N-Methyl-N-(((R)-5-(4-methylpiperazin-1-yl)-1,2,3,4-tetrahydroisoquinolin-3-yl)methyl)-5,6,7,8-tetrahydroquinolin-8-amine (**25e**). Compound **25e** was synthesized by a two-step sequence (general procedure D → general procedure A). White foam (69 % yield over two steps). ^{1}H NMR (400 MHz, $CDCl_3$): δ 8.42 (dd, J = 4.8, 1.7 Hz, 1H), 7.36 - 7.28 (m, 1H), 7.10 - 6.99 (m, 2H), 6.86 (dd, J = 7.9, 1.2 Hz, 1H), 6.73 (dd, J = 7.6, 1.1 Hz, 1H), 4.07 (d, J = 15.4 Hz, 1H), 3.98 - 3.87 (m, 2H), 3.00 (dt, J = 10.2, 4.6 Hz, 2H), 2.85 - 2.45 (m, 15H), 2.37 - 2.14 (m, 5H), 2.06 - 1.87 (m, 3H), 1.68 (dddd, J = 15.5, 10.3, 7.2, 4.8 Hz, 1H). ^{13}C NMR (101 MHz, $CDCl_3$): δ 158.1, 151.3, 146.8, 136.8, 135.9, 133.9, 129.7, 126.1, 121.7, 121.6, 116.9, 64.5, 59.7, 55.7, 53.5, 51.7, 48.2, 46.2, 41.1, 29.7, 29.2, 26.1, 21.3. HRMS (*m/z*): calculated for $[C_{25}H_{35}N_5 + H]^+$: 406.29707, found: 406.29649.

(S)-N-(((R)-5-(4-Ethylpiperazin-1-yl)-1,2,3,4-tetrahydroisoquinolin-3-yl)methyl)-N-methyl-5,6,7,8-tetrahydroquinolin-8-amine (**25f**). Compound **25f** was synthesized by a two-step sequence (general procedure D → general procedure A). White foam (61 % yield over two steps). ^{1}H NMR (400 MHz, $CDCl_3$): δ 8.45 (dd, J = 4.8, 1.7 Hz, 1H), 7.39 - 7.32 (m, 1H), 7.12 - 7.05 (m, 2H), 6.90 (dd, J = 7.9, 1.2 Hz, 1H), 6.77 (dd, J = 7.6, 1.1 Hz, 1H), 4.13 (d, J = 15.5 Hz, 1H), 4.02 - 3.95 (m, 2H), 3.05 (dd, J = 11.7, 5.0 Hz, 2H), 2.89 - 2.45 (m, 18H), 2.40 - 2.23 (m, 1H), 2.08 - 1.92 (m, 3H), 1.78 - 1.67 (m, 1H), 1.12 (t, J = 7.2 Hz, 3H). ^{13}C NMR (101 MHz, $CDCl_3$): δ 158.0, 151.2, 146.7, 136.5, 136.4, 133.6, 129.8, 125.9, 121.5, 121.4, 116.6, 64.3, 59.7,

53.3, 52.3, 51.5, 51.5, 48.5, 41.5, 30.0, 29.1, 26.1, 21.2, 12.0. HRMS (*m/z*): calculated for $[C_{26}H_{37}N_5 + H]^+$: 420.31272, found: 420.31300.

(S)-N-(((R)-5-(4-Isopropylpiperazin-1-yl)-1,2,3,4-tetrahydroisoquinolin-3-yl)methyl)-N-methyl-5,6,7,8-tetrahydroquinolin-8-amine (**25g**). Compound **25g** was synthesized by a two-step sequence (general procedure D → general procedure A). Light yellow foam (55 % yield over two steps). ^{1}H NMR (400 MHz, $CDCl_3$): δ 8.39 (dd, J = 4.7, 1.7 Hz, 1H), 7.29 - 7.23 (m, 1H), 7.04 - 6.95 (m, 2H), 6.81 (d, J = 7.9 Hz, 1H), 6.68 (d, J = 7.6 Hz, 1H), 4.00 (d, J = 15.4 Hz, 1H), 3.92 - 3.82 (m, 2H), 3.01 - 2.44 (m, 19H), 2.12 (dd, J = 16.3, 10.5 Hz, 1H), 1.99 - 1.83 (m, 3H), 1.65 (s, 1H), 1.02 (d, J = 6.7 Hz, 6H). ^{13}C NMR (101 MHz, $CDCl_3$): δ 158.0, 151.3, 146.7, 136.6, 136.3, 133.7, 129.8, 125.9, 121.5, 121.4, 116.6, 64.4, 59.7, 54.4, 51.9, 51.5, 49.2, 48.5, 41.4, 30.0, 29.1, 26.2, 21.2, 18.8, 18.6. HRMS (*m/z*): calculated for $[C_{27}H_{39}N_5 + H]^+$: 434.32837, found: 434.32803.

(S)-N-(((R)-5-(4-Cyclopropylpiperazin-1-yl)-1,2,3,4-tetrahydroisoquinolin-3-yl)methyl)-N-methyl-5,6,7,8-tetrahydroquinolin-8-amine (**25h**). Compound **25h** was synthesized by a two-step sequence (general procedure D → general procedure A). White foam (54 % yield over two steps). ^{1}H NMR (400 MHz, $CDCl_3$): δ 8.46 (dd, J = 4.8, 1.7 Hz, 1H), 7.36 (ddd, J = 7.6, 1.8, 0.9 Hz, 1H), 7.12 - 7.04 (m, 2H), 6.87 (dd, J = 7.9, 1.1 Hz, 1H), 6.76 (dd, J = 7.6, 1.1 Hz, 1H), 4.13 (d, J = 15.4 Hz, 1H), 3.99 (q, J = 8.6 Hz, 2H), 3.01 - 2.62 (m, 15H), 2.48 (s, 3H), 2.35 - 2.26 (m, 1H), 2.09 - 1.91 (m, 3H), 1.75 - 1.63 (m, 2H), 0.49 - 0.42 (m, 4H). ^{13}C NMR (101 MHz, $CDCl_3$): δ 158.0, 151.4, 146.7, 136.6, 136.4, 133.7, 129.9, 125.9, 121.6, 121.4, 116.7, 64.4, 59.8, 53.8, 51.5, 48.6, 41.5, 38.5, 30.1, 29.2, 26.2, 21.3, 5.7. HRMS (*m/z*): calculated for $[C_{27}H_{37}N_5 + H]^+$: 432.31272, found: 432.31173.

(S)-N-Methyl-N-(((R)-5-(4-(oxetan-3-yl)piperazin-1-yl)-1,2,3,4-tetrahydroisoquinolin-3-yl)methyl)-5,6,7,8-tetrahydroquinolin-8-amine (**25i**). Compound **25i** was synthesized by a two-step sequence (general procedure D → general procedure A). White foam (63 % yield over two steps). ^{1}H NMR (400 MHz, $CDCl_3$): δ 8.46 (dd, J = 4.7, 1.7 Hz, 1H), 7.40 - 7.32 (m, 1H), 7.15 - 7.04 (m, 2H), 6.90 (dd, J = 7.8, 1.2 Hz, 1H), 6.78 (dd, J = 7.6, 1.1 Hz, 1H), 4.70 - 4.64 (m, 4H), 4.11 (d, J = 15.5 Hz, 1H), 3.97 (q, J = 8.1 Hz, 2H), 3.58 (q, J = 6.5 Hz, 1H), 3.05 (dt, J = 10.5, 4.3 Hz, 2H), 2.86 - 2.40 (m, 16H), 2.24 (s, 1H), 2.08 - 1.91 (m, 3H), 1.78 - 1.67 (m, 1H). ^{13}C NMR (101 MHz, $CDCl_3$): δ 157.9, 150.9, 146.6, 136.5, 136.5, 133.6, 129.8, 125.9, 121.7, 121.3, 116.6, 75.3, 64.2, 59.6, 59.1, 51.4, 51.1, 50.0, 48.5, 41.5, 30.0, 29.0, 26.2, 21.1. HRMS (*m/z*): calculated for $[C_{27}H_{37}N_5O + H]^+$: 448.30764, found: 448.30681.

(S)-N-Methyl-N-(((R)-5-(4-(3-(trifluoromethyl)phenyl)piperazin-1-yl)-1,2,3,4-tetrahydroisoquinolin-3-yl)methyl)-5,6,7,8-tetrahydroquinolin-8-amine (**25j**). Compound **25j** was synthesized by a two-step sequence (general procedure D → general procedure A). Light yellow foam (53 % yield over two steps). ^{1}H NMR (399 MHz, $CDCl_3$): δ 8.46 (dd, J = 4.8, 1.7 Hz, 1H), 7.39 - 7.29 (m, 2H), 7.16 - 7.01 (m, 5H), 6.90 (d, J = 7.8 Hz, 1H), 6.80 (d, J = 7.6 Hz, 1H), 4.08 (d, J = 15.4 Hz, 1H), 4.01 - 3.90 (m, 2H), 3.33 (dt, J = 31.4, 10.7 Hz, 5H), 3.15 (ddd, J = 10.3, 6.2, 3.7 Hz, 2H), 2.91 - 2.74 (m, 6H), 2.66 (dt, J = 16.6, 4.6 Hz, 1H), 2.52 (s, 4H), 2.21 (dd, J = 16.3, 10.4 Hz, 1H), 1.99 (dddd, J = 29.6, 22.0, 11.3, 3.3 Hz, 3H), 1.75 - 1.62 (m, 1H). ^{13}C NMR (101 MHz, $CDCl_3$): δ 158.0, 151.5, 150.9, 146.8, 136.8, 136.7, 133.8, 131.8, 131.5, 131.2, 130.9, 129.9, 129.5, 128.4, 126.1, 125.7, 123.0, 122.1, 121.5, 120.3, 118.8, 118.8, 116.7, 115.8, 115.8, 115.8, 112.1, 112.1, 112.0, 112.0, 64.5, 59.8, 51.6, 51.6, 49.2, 48.7, 41.4, 30.2, 29.3, 26.0, 21.4. ^{19}F NMR (376 MHz, $CDCl_3$, TFA standard): δ 13.3. HRMS (*m/z*): calculated for $[C_{31}H_{36}F_3N_5 + H]^+$: 536.30011, found: 536.29919.

(S)-N-Methyl-N-(((R)-5-(4-(pyridin-2-yl)piperazin-1-yl)-1,2,3,4-tetrahydroisoquinolin-3-yl)methyl)-5,6,7,8-tetrahydroquinolin-8-amine (**25k**). Compound **25k** was synthesized by a two-step sequence (general procedure D → general procedure A). White foam (47 % yield over two steps). ^{1}H NMR (400 MHz, $CDCl_3$): δ 8.43 (dd, J = 4.7, 1.8 Hz, 1H), 8.17 (dd, J = 5.0, 1.9 Hz, 1H), 7.44 (ddd, J = 8.9, 7.1, 2.0 Hz, 1H), 7.29 (dd, J = 7.8, 1.7 Hz, 1H), 7.11 - 6.96 (m, 2H), 6.84 (d, J = 7.9 Hz, 1H), 6.75 (d, J = 7.6 Hz, 1H), 6.64 (d, J = 8.6 Hz, 1H), 6.59 (dd, J = 7.1, 5.0 Hz, 1H), 4.04 (d, J = 15.4 Hz, 1H), 3.99 - 3.84 (m, 2H), 3.60 (d, J = 33.1 Hz, 4H), 3.07 (dt, J = 10.4, 4.5 Hz, 2H), 2.90 - 2.44 (m, 11H), 2.19 (dd, J = 16.4, 10.4 Hz, 1H), 2.07 - 1.86 (m, 3H), 1.72 - 1.60 (m, 1H). ^{13}C NMR (101 MHz, $CDCl_3$): δ 159.6, 158.0, 151.1, 147.9, 146.8, 137.4, 136.7, 136.6, 133.7, 129.9, 126.0, 121.9, 121.5, 116.6, 113.3, 107.1, 64.4, 59.7, 51.5, 48.6, 45.8, 41.8, 30.2, 29.2, 26.3, 21.3. HRMS (*m/z*): calculated for $[C_{29}H_{36}N_6 + H]^+$: 469.30797, found: 469.30711.

(S)-N-Methyl-N-(((R)-5-(4-(pyrimidin-2-yl)piperazin-1-yl)-1,2,3,4-tetrahydroisoquinolin-3-yl)methyl)-5,6,7,8-tetrahydroquinolin-8-amine (**25l**). Compound **25l** was synthesized by a two-step sequence (general procedure D → general procedure A). Light yellow foam (39 % yield over two steps). ^{1}H NMR (400 MHz, $CDCl_3$): δ 8.43 (d, J = 4.6 Hz, 1H), 8.28 (t, J = 4.6 Hz, 2H), 7.29 (d, J = 7.7 Hz, 1H), 7.07 - 6.97 (m, 2H), 6.81 (d, J = 7.9 Hz, 1H), 6.74 (d, J = 7.6 Hz, 1H), 6.44 (t, J = 4.8 Hz, 1H), 4.20 - 3.69 (m, 7H), 2.99 (dq, J = 12.2, 7.2, 5.9 Hz, 2H), 2.89 (dd, J = 16.3, 3.0 Hz, 1H), 2.81 - 2.59 (m, 6H), 2.57 - 2.40 (m, 4H), 2.19 (dd, J = 16.2, 10.2 Hz, 1H), 2.06 - 1.88 (m, 3H), 1.67 (h, J = 9.4 Hz, 1H). ^{13}C NMR (101 MHz, $CDCl_3$): δ 161.7, 158.1, 157.7, 151.2, 146.8, 136.7, 136.6, 133.8, 130.0, 126.0, 122.0, 121.5, 116.7, 109.8, 64.4, 59.7, 51.7, 51.6, 48.7, 44.3, 41.7, 30.2, 29.2, 26.3, 21.3. HRMS (*m/z*): calculated for $[C_{28}H_{35}N_7 + H]^+$: 470.30322, found: 470.30297.

(S)-N-Methyl-N-(((R)-5-(4-(pyridin-2-ylmethyl)piperazin-1-yl)-1,2,3,4-tetrahydroisoquinolin-3-yl)methyl)-5,6,7,8-tetrahydroquinolin-8-amine (**25m**). Compound **25m** was synthesized by a two-step sequence (general procedure D → general procedure A). White foam (38 % yield over two steps). ^{1}H NMR (400 MHz, $CDCl_3$): δ 8.50 (d, J = 4.9 Hz, 1H), 8.40 (d, J = 4.6 Hz, 1H), 7.58 (td, J = 7.6, 1.8 Hz, 1H), 7.37 (d, J = 7.8 Hz, 1H), 7.25 (s, 1H), 7.08 (dd, J = 7.4, 5.1 Hz, 1H), 7.03 - 6.96 (m, 2H), 6.80 (d, J = 7.9 Hz, 1H), 6.68 (d, J = 7.6 Hz, 1H), 4.00 (d, J = 15.4 Hz, 1H), 3.91 - 3.82 (m, 2H), 3.69 - 3.64 (m, 2H), 2.99 (dt, J = 10.0, 4.1 Hz, 2H), 2.80 - 2.41 (m, 16H), 2.10 (dd, J = 16.5, 10.2 Hz, 1H), 2.01 - 1.84 (m, 3H), 1.67 - 1.58 (m, 1H). ^{13}C NMR (101 MHz, $CDCl_3$): δ 158.5, 158.0, 151.3, 149.2, 146.7, 136.6, 136.3, 136.3, 133.7, 129.7, 125.9, 123.2, 121.9, 121.5, 121.5, 116.6, 110.0, 64.7, 64.4, 59.6, 53.8, 51.5, 48.5, 41.6, 30.0, 29.2, 26.2, 21.3. HRMS (*m/z*): calculated for $[C_{30}H_{38}N_6 + H]^+$: 483.32362, found: 483.32315.

(S)-N-Methyl-N-(((R)-5-((3R,5S)-3,4,5-trimethylpiperazin-1-yl)-1,2,3,4-tetrahydroisoquinolin-3-yl)methyl)-5,6,7,8-tetrahydroquinolin-8-amine (**25n**). Compound **25n** was synthesized by a two-step sequence (general procedure D → general procedure A). Light yellow foam (55 % yield over two steps). ^{1}H NMR (400 MHz, $CDCl_3$): δ 8.38 (dd, J = 4.7, 1.7 Hz, 1H), 7.33 - 7.20 (m, 1H), 7.06 - 6.91 (m, 2H), 6.76 (d, J = 7.9 Hz, 1H), 6.66 (d, J = 7.6 Hz, 1H), 3.99 (d, J = 15.4 Hz, 1H), 3.91 - 3.79 (m, 2H), 2.88 - 2.54 (m, 8H), 2.44 (s, 4H), 2.33 - 2.09 (m, 7H), 2.01 - 1.83 (m, 3H), 1.65 (t, J = 6.4 Hz, 1H), 1.02 (dd, J = 25.3, 6.2 Hz, 6H). ^{13}C NMR (101 MHz, $CDCl_3$): δ 158.0, 150.8, 146.7, 136.6, 136.2, 133.7, 129.6, 126.0, 121.6, 121.4, 116.5, 64.3, 59.9, 59.7, 58.8, 58.4, 58.1, 51.6, 48.4, 41.3, 37.9, 29.9, 29.1, 26.0, 21.2, 18.1, 18.0. HRMS (*m/z*): calculated for $[C_{27}H_{39}N_5 + H]^+$: 434.32837, found: 434.32964.

(S)-N-(((R)-5-((R)-Hexahydropyrrolo[1,2-a]pyrazin-2(1H)-yl)-1,2,3,4-tetrahydroisoquinolin-3-yl)methyl)-N-methyl-5,6,7,8-tetrahydroquinolin-8-amine (**25o**). Compound **25o** was synthesized by a two-step sequence (general procedure D → general procedure A). White foam (53 % yield over two steps). ^{1}H NMR (400 MHz, $CDCl_3$): δ 8.38 (dd, J = 4.8, 1.7 Hz, 1H), 7.24 (dd, J = 7.7, 1.7 Hz, 1H), 7.04 - 6.91 (m, 2H), 6.83 (d, J = 7.8 Hz, 1H), 6.67 (d, J = 7.6 Hz, 1H), 3.97 (d, J = 15.4 Hz, 1H), 3.91 - 3.76 (m, 2H), 3.09 - 2.96 (m, 4H), 2.75 (tdd, J = 26.2, 11.2, 4.4 Hz, 5H), 2.57 (dd, J = 16.6, 4.8 Hz, 1H), 2.52 - 2.37 (m, 4H), 2.31 - 2.09 (m, 5H), 2.01 - 1.55 (m, 8H), 1.31 (tt, J = 10.9, 4.6 Hz, 1H). ^{13}C NMR (101 MHz, $CDCl_3$): δ 157.8, 151.3, 146.6, 136.5, 136.4, 133.6, 129.9, 125.8, 121.6, 121.3, 117.1, 64.3, 62.7, 59.8, 56.8, 53.2, 51.9, 51.4, 50.5, 48.5, 40.9, 29.9, 29.0, 27.1, 25.6, 21.2, 21.1. HRMS (*m/z*): calculated for $[C_{27}H_{37}N_5 + H]^+$: 432.31272, found: 432.31206.

(S)-N-(((R)-5-((S)-Hexahydropyrrolo[1,2-a]pyrazin-2(1H)-yl)-1,2,3,4-tetrahydroisoquinolin-3-yl)methyl)-N-methyl-5,6,7,8-tetrahydroquinolin-8-amine (**25p**). Compound **25p** was synthesized by a two-step sequence (general procedure D → general procedure A). White foam (57 % yield over two steps). ^{1}H NMR (400 MHz, $CDCl_3$): δ 8.35 (dd, J = 4.8, 1.7 Hz, 1H), 7.21 (dd, J = 7.7, 1.7 Hz, 1H), 7.00 - 6.88 (m, 2H), 6.78 (d, J = 7.9 Hz, 1H), 6.63 (d, J = 7.6 Hz, 1H), 3.96 (d, J = 15.5 Hz, 1H), 3.87 - 3.78 (m, 2H), 2.95 (dddd, J = 26.7, 13.1, 6.7, 2.2 Hz, 4H), 2.77 - 2.59 (m, 5H), 2.58 - 2.49 (m, 2H), 2.46 - 2.33 (m, 4H), 2.29 (td, J = 10.9, 3.1 Hz, 1H), 2.07 (ddp, J = 15.1, 10.4, 5.6, 5.1 Hz, 3H), 1.96 - 1.54 (m, 8H), 1.36 (dq, J = 15.6, 5.0 Hz, 1H). ^{13}C NMR (101 MHz, $CDCl_3$): δ 157.7, 151.1, 146.5, 136.4, 136.3, 133.5, 129.7, 125.7, 121.4, 121.2, 116.9, 64.2, 62.8, 59.7, 55.8, 53.2, 51.8, 51.4, 51.3, 48.4, 40.9, 29.9, 29.0, 27.2, 25.6, 21.0. HRMS (*m/z*): calculated for $[C_{27}H_{37}N_5 + H]^+$: 432.31272, found: 432.31401.

tert-Butyl (R)-5-(4-((benzyloxy)carbonyl)piperazin-1-yl)-3-((methyl((S)-5,6,7,8-tetrahydroquinolin-8-yl)amino)methyl)-3,4-dihydroisoquinoline-2(1H)-carboxylate (**26**). Compound **26** was obtained according to general procedure D using **23** (250 mg, 0.514 mmol), $Pd_2(dba)_3$ (24 mg, 0.026 mmol), *rac*-BINAP (48 mg, 0.077 mmol), cesium carbonate (234 mg, 0.720 mmol), degassed toluene (2.5 mL), and benzyl piperazine-1-carboxylate (liquid) (0.136 mg, 0.617 mmol). Yellow foamy solid (228 mg, 71 % yield). ^{1}H NMR (400 MHz, $CDCl_3$): δ 8.25 (s, 1H), 7.46 - 7.28 (m, 6H), 7.08 (t, J = 7.8 Hz, 1H), 6.99 (s, 1H), 6.81 (d, J = 7.9 Hz, 1H), 6.77 - 6.60 (m, 1H), 5.17 (s, 2H), 4.72 - 4.27 (m, 2H), 3.73 (dd, J = 110.2, 23.1 Hz, 6H), 3.23 (d, J = 16.1 Hz, 1H), 2.96 (s, 2H), 2.88 - 2.55 (m, 6H), 2.49 - 2.30 (m, 1H), 2.26 (s, 3H), 1.92 (dd, J = 45.1, 9.7 Hz, 3H), 1.49 (s, 10H). HRMS calculated for $[C_{37}H_{47}N_5O_4 + H]^+$: 626.37063, found: 626.37010.

Benzyl 4-((R)-3-((methyl((S)-5,6,7,8-tetrahydroquinolin-8-yl)amino)methyl)-1,2,3,4-tetrahydroisoquinolin-5-yl)piperazine-1-carboxylate (**27**). Compound **27** was obtained according to general procedure A. Light yellow foam (90 % yield). ^{1}H NMR (400 MHz, $CDCl_3$): δ 8.41 (dd, *J* = 4.8, 1.7 Hz, 1H), 7.38 – 7.33 (m, 6H), 7.16 – 7.08 (m, 2H), 6.88 (dd, *J* = 8.0, 1.1 Hz, 1H), 6.82 (dd, *J* = 7.7, 1.1 Hz, 1H), 5.16 (s, 2H), 4.28 (d, *J* = 15.6 Hz, 1H), 4.10 (dd, *J* = 15.5, 5.7 Hz, 2H), 3.10 – 2.88 (m, 8H), 2.84 – 2.58 (m, 7H), 2.36 (s, 3H), 2.11 – 1.87 (m, 4H), 1.75 (s, 1H). HRMS calculated for $[C_{32}H_{39}N_5O_2 + H]^+$: 526.31820, found: 526.31704.

Benzyl 4-((R)-2-methyl-3-((methyl((S)-5,6,7,8-tetrahydroquinolin-8-yl)amino)methyl)-1,2,3,4-tetrahydroisoquinolin-5-yl)piperazine-1-carboxylate (**28**). To a 20-mL scintillation vial equipped with a magnetic stir bar was charged with **27** (336 mg, 0.639 mmol), sodium triacetoxyborohydride (406 mg, 1.92 mmol), dichloromethane (6.4 mL). After stirring for 5

minutes, paraformaldehyde (58 mg, 1.92 mmol) was added in one portion. The resulting mixture was stirred at room temperature for 48 hours. Upon the completion of the reaction as judged by TLC and LCMS, the mixture was quenched by addition of saturated $NaHCO_3$ solution. The biphasic mixture was transferred to a separatory funnel. The aqueous layer was separated and extracted with DCM (3 times). The combined organic extract was dried over anhydrous sodium sulfate and concentrated under reduced pressure to a crude material which was purified by CombiFlash system (24g silica column, 5 minutes DCM → 30 minutes 0-30% 8:2:0.6 DCM/MeOH/NH_3 solution, 7N in MeOH) to afford the title compound as a yellow gel (410 mg, quantitative yield). ^{1}H NMR (400 MHz, $CDCl_3$): δ 8.46 - 8.37 (m, 1H), 7.41 - 7.30 (m, 6H), 7.10 (t, J = 7.7 Hz, 1H), 7.02 (dd, J = 7.7, 4.7 Hz, 1H), 6.84 (d, J = 7.9 Hz, 1H), 6.77 (d, J = 7.6 Hz, 1H), 5.17 (s, 2H), 3.84 - 3.61 (m, 7H), 2.88 (t, J = 25.2 Hz, 8H), 2.67 (dd, J = 16.7, 5.3 Hz, 2H), 2.48 (d, J = 23.7 Hz, 4H), 2.30 (s, 3H), 1.95 (s, 3H), 1.65 (dt, J = 9.2, 4.8 Hz, 1H). HRMS calculated for $[C_{33}H_{41}N_5O_2 + H]^+$: 540.33385, found: 540.33370.

(S)-N-Methyl-N-(((R)-2-methyl-5-(piperazin-1-yl)-1,2,3,4-tetrahydroisoquinolin-3-yl)methyl)-5,6,7,8-tetrahydroquinolin-8-amine (**29**). To a 20-mL scintillation vial equipped with a Teflon-coated magnetic stir bar was charged with **28** (410 mg, 0.760 mmol) and trifluoroacetic acid (3.8 mL). Trifluoromethanesulfonic acid (202 μL, 2.28 mmol) was added dropwise at 0 °C, and the resulting mixture was stirred at room temperature for 1 hour. Upon the completion of the reaction as judged by LCMS, the mixture was diluted with DCM, cooled in an ice-bath, and carefully quenched by the addition of 3N NaOH until pH>12. The biphasic mixture was transferred to a separatory funnel. The aqueous layer was separated and extracted with DCM (3 times). The combined organic extract was dried over anhydrous sodium sulfate and concentrated under reduced pressure to a crude material which was purified by CombiFlash

system (12g silica column, 5 minutes DCM → 30 minutes 0-80% 8:2:0.6 DCM/MeOH/NH_3 solution, 7N in MeOH) to afford the title compound as a light yellow foam (193 mg, 63 % yield). ^{1}H NMR (400 MHz, $CDCl_3$): δ 8.44 (td, J = 4.5, 1.6 Hz, 1H), 7.38 - 7.30 (m, 1H), 7.12 (t, J = 7.7 Hz, 1H), 7.05 (ddd, J = 7.4, 4.8, 2.6 Hz, 1H), 6.95 - 6.86 (m, 1H), 6.81 - 6.72 (m, 1H), 4.23 (s, 1H), 3.90 - 3.77 (m, 3H), 3.13 (t, J = 4.8 Hz, 3H), 3.02 - 2.78 (m, 8H), 2.74 - 2.44 (m, 7H), 2.29 (s, 3H), 2.07 - 1.86 (m, 3H), 1.73 - 1.61 (m, 1H). ^{13}C NMR (101 MHz, $CDCl_3$): δ 157.8, 151.7, 146.7, 136.7, 136.0, 133.8, 129.6, 125.9, 121.5, 121.3, 116.5, 64.5, 62.1, 59.8, 52.2, 51.5, 51.1, 48.2, 41.7, 40.6, 29.7, 29.3, 29.2, 28.9, 25.4, 21.2. HRMS calculated for $[C_{25}H_{35}N_5 + H]^+$: 406.29707, found: 406.29641.

(S)-N-Methyl-N-(((R)-2-methyl-5-(4-methylpiperazin-1-yl)-1,2,3,4-tetrahydroisoquinolin-3-yl)methyl)-5,6,7,8-tetrahydroquinolin-8-amine (**30**). Compound **30** was prepared according to the procedure described for the synthesis of **28** using **12a** (96 mg, 0.245 mmol), dichloromethane (2.5 mL), sodium triacetoxyborohydride (156 mg, 0.734 mmol), and paraformaldehyde (37 mg, 1.22 mmol). Yellow amorphous solid (74.2 mg, 72 % yield). ^{1}H NMR (400 MHz, $CDCl_3$): *δ* 8.40 (dd, J = 4.8, 1.7 Hz, 1H), 7.30 - 7.23 (m, 1H), 7.07 - 6.95 (m, 2H), 6.84 (dd, J = 8.0, 1.2 Hz, 1H), 6.71 - 6.65 (m, 1H), 3.78 - 3.63 (m, 3H), 2.88 - 2.75 (m, 7H), 2.65 - 2.45 (m, 7H), 2.39 (s, 3H), 2.33 (s, 3H), 2.27 (s, 3H), 2.04 - 1.80 (m, 4H), 1.61 (tdd, J = 10.9, 5.6, 3.2 Hz, 1H). ^{13}C NMR (101 MHz, $CDCl_3$): *δ* 157.8, 151.4, 146.6, 136.5, 135.2, 133.8, 129.1, 126.0, 121.5, 121.5, 116.8, 65.1, 57.1, 56.5, 55.8, 55.6, 51.7, 46.2, 40.7, 39.6, 28.7, 27.1, 25.9, 20.2. HRMS (*m/z*): calculated for $[C_{26}H_{37}N_5 + H]^+$: 420.31272, found: 420.31212.

2-(tert-Butyl) 3-methyl (R)-5-(4-methylpiperazin-1-yl)-3,4-dihydroisoquinoline-2,3(1H)-dicarboxylate (**31**). Compound **31** was prepared according to the procedure described for the preparation of **8** using compound **13** (0.4 g, 1.08 mmol), 1-methylpiperazine (144 µL, 1.30

mmol), $Pd_2(dba)_3$ (49 mg, 0.054 mmol), *rac*-BINAP (101 mg, 0.162 mmol), cesium carbonate (493 mg, 1.51 mmol), and toluene (5.40 mL). Orange amorphous solid (204 mg, 49 % yield). ^{1}H NMR (400 MHz, $CDCl_3$): δ 7.13 (dq, J = 8.1, 4.3 Hz, 1H), 7.00 - 6.74 (m, 2H), 5.02 (dt, J = 6.5, 3.3 Hz, 0.5H), 4.76 - 4.55 (m, 1.5H), 4.42 (ddd, J = 37.7, 16.1, 2.5 Hz, 1H), 3.64 - 3.44 (m, 3H), 3.14 (tdd, J = 18.6, 14.3, 6.4 Hz, 1H), 2.91 - 2.81 (m, 3H), 2.57 (s, 3H), 2.34 (d, J = 3.9 Hz, 3H), 1.45 (dt, J = 31.9, 2.5 Hz, 9H). MS (m/z): 390 ($M+H^+$).

tert-Butyl (R)-3-formyl-5-(4-methylpiperazin-1-yl)-3,4-dihydroisoquinoline-2(1H)-carboxylate (**32**). Compound **32** was prepared from ester **31** according to the procedure described for the synthesis of **9**. The crude material was used for the next step without purification. ^{1}H NMR (400 MHz, $CDCl_3$): δ 9.48 – 9.22 (m, 1H), 7.07 (dt, *J* = 8.7, 4.3 Hz, 1H), 6.81 (ddt, *J* = 36.5, 17.5, 8.9 Hz, 2H), 4.81 – 4.17 (m, 2H), 3.52 – 3.04 (m, 1H), 2.97 – 2.71 (m, 4H), 2.51 (s, 4H), 2.27 (d, *J* = 10.1 Hz, 3H), 1.57 – 1.19 (m, 9H).

tert-Butyl (R)-3-(((4aR,10bS)-3,4,4a,5,6,10b-hexahydro-1,10-phenanthrolin-1(2H)-yl)methyl)-5-(4-methylpiperazin-1-yl)-3,4-dihydroisoquinoline-2(1H)-carboxylate (**34**). To a solution of aldehyde **32** (365 mg, 1.01 mmol) and amine **33** (210 mg, 1.12 mmol) in dichloromethane (5 mL) was added sodium triacetoxyborohydride (445 mg, 2.1 mmol). The reaction was stirred overnight (16 hours) at room temperature, followed by addition of **33** (100 mg, 0.53 mmol) and sodium triacetoxyborohydride (220 mg, 1.04 mmol). The reaction was stirred for an additional 16 hours. The organics were washed with saturated $NaHCO_3$ and brine solutions then separated and dried over anhydrous Na_2SO_4. Filtration and concentration followed by column chromatography (DCM/MeOH (0.1% NH_4OH) gradient) gave the title compound as a white foam (388 mg, 72 % yield). ^{1}H NMR (400MHz, $CDCl_3$): δ 1.48 (s, 9H), 1.63 (m, 2H), 1.89

(m, 2H), 2.39 (d, 4H, *J*=5 Hz), 2.66 (m, 10H), 3.01 (m, 4H), 3.25 (m, 2H), 4.27 (d, 1H, *J*=18 Hz), 4.4 (d, 1H, J=18 Hz), 4.54 (d, 1H, J=18 Hz), 4.65 (m, 1H), 6.2 (d, 0.5H, J=7 Hz), 6.29 (d, 0.5H, J=8 Hz), 6.74 (d, 1H, *J*=6 Hz), 6.97 (m, 2H), 7.41 (d, 1H, *J*=8 Hz), 7.93 (d, 1H, *J*=15 Hz); MS (m/z): 532 ($M+H^+$).

(4aR,10bS)-1-(((R)-5-(4-Methylpiperazin-1-yl)-1,2,3,4-tetrahydroisoquinolin-3-yl)methyl)-1,2,3,4,4a,5,6,10b-octahydro-1,10-phenanthroline (**35**). Compound **35** was obtained according to general procedure A. Off-white foam (79 % yield). ^{1}H NMR (400MHz, $CDCl_3$): δ 1.69 (m, 6H), 2.11 9m, 1H), 2.24 (m, 3H), 2.34 (s, 3H), 2.51 (m, 4H), 2.73 (m, 6H), 2.97 (m, 6H), 3.61 (m, 1H), 4.04 (m, 2H), 6.69 (d, 1H, J=8Hz), 6.85 (d, 1H, J=7Hz), 7.08 (m, 2H), 7.39 (d, 1H, J=8Hz), 8.36 (d, 1H, J=5Hz). ^{13}C NMR (125 MHz, $CDCl_3$): δ 21.88, 23.65, 26.97, 28.61, 29.28, 33.7, 46.22, 46.3, 51.63, 52.55, 55.56, 55.69, 58.57, 66.83, 117.05, 121.59, 122.47,126.14, 130.08, 133.6, 137.17, 146.11, 147.15, 151.31, 157.61. HRMS calculated for $[C_{27}H_{38}N_5 + H]^+$: 432.31272, found: 432.31169.

ASSOCIATED CONTENT

Supporting Information.

The synthetic preparation of amines S1-S4 used in Scheme 3, details for the 3D QSAR model used in Figure 3, docking methodology used in Figure 4 and molecular formula strings with accompanying biological data (CSV) are provided

AUTHOR INFORMATION

Corresponding Authors

E-mail: dliotta@emory.edu, ljwilso@emory.edu

Author Contributions

The manuscript was written by HHN and through the contributions of all authors. Compounds were synthesized by HHN, RJW and LJW. CJB and MBK performed the modeling studies. All authors have given approval to the final version of the manuscript.

Funding Sources

The authors acknowledge the use of shared instrumentation provided by grants from NSF (CHE1531620).

Notes

DCL is the principle investigator on a research grant from Bristol-Myers Squibb Research and Development to Emory University. DCL, LJW, EJM, EJ, HHN, YAT, RJW, VTT, and MBK are co-inventors on Emory-owned Intellectual Property that includes CXCR4 antagonists.

ACKNOWLEDGMENT

The authors are grateful to Dr. Fred Strobel and Ms. Samantha Summer for assistance in the collection of HRMS data. We also thank Dr. Sameshnee Pelly for managing intellectual property and Dr. Manohar T. Saindane for the scale-up production of bromide **23**.

ABBREVIATIONS

CXCR4, chemokine (C-X-C motif) receptor 4; GPCR, G protein-coupled receptor; CXCL12, CXC chemokine ligand type 12; THQ, 5,6,7,8-tetrahydroquinoline; TIQ, 1,2,3,4-tetrahydroisoquinoline; IC_{50}, 50% inhibitory concentration; CYP 450, cytochrome P450; *h*ERG, the human ether-a-go-go related gene; Caco, human colorectal adenocarcinoma cells; PAMPA, parallel artificial membrane permeability assay; HLM, human liver microsomes; MLM, mouse liver microsomes; SAR, structure-activity relationship; $T_{1/2}$, half-life; LC, liquid chromatography; HPLC, high pressure liquid chromatography; MS, mass spectrometry; HRMS, high resolution mass spectrometry; TLC, thin layer chromatography; Bz, benzoyl; MeOH, methanol; EtOH, ethanol; Et_3N, triethylamine; THF, tetrahydrofuran; EtOAc, ethyl acetate; Na_2SO_4, sodium sulfate; K_2CO_3, potassium carbonate; Na_2CO_3, sodium carbonate; CH_2Cl_2 or DCM, methylene chloride; $NaHCO_3$, sodium bicarbonate; HCl, hydrochloric acid.

REFERENCES

1. Zou, Y.-R.; Kottmann, A. H.; Kuroda, M.; Taniuchi, I.; Littman, D. R. Function of the Chemokine Receptor CXCR4 in Haematopoiesis and in Cerebellar Development. *Nature* **1998**, *393*, 595-599.

2. Allen, S. J.; Crown, S. E.; Handel, T. M. Chemokine: Receptor Structure, Interactions, and Antagonism. *Annu Rev Immunol* **2007**, *25*, 787-820.

3. Tachibana, K.; Hirota, S.; Iizasa, H.; Yoshida, H.; Kawabata, K.; Kataoka, Y.; Kitamura, Y.; Matsushima, K.; Yoshida, N.; Nishikawa, S.-i.; Kishimoto, T.; Nagasawa, T. The Chemokine Receptor CXCR4 is Essential for Vascularization of the Gastrointestinal Tract. *Nature* **1998**, *393*, 591-594.

4. Balkwill, F. Cancer and the Chemokine Network. *Nat Rev Cancer* **2004**, *4*, 540-550.

5. Shirozu, M.; Nakano, T.; Inazawa, J.; Tashiro, K.; Tada, H.; Shinohara, T.; Honjo, T. Structure and Chromosomal Localization of the Human Stromal Cell-Derived Factor 1 (SDF1) gene. *Genomics* **1995**, *28*, 495-500.

6. Choi, W. T.; Duggineni, S.; Xu, Y.; Huang, Z.; An, J. Drug Discovery Research Targeting the CXC Chemokine Receptor 4 (CXCR4). *J Med Chem* **2012**, *55*, 977-994.

7. (a) Bleul, C. C.; Farzan, M.; Choe, H.; Parolin, C.; Clark-Lewis, I.; Sodroski, J.; Springer, T. A. The Lymphocyte Chemoattractant SDF-1 is a Ligand for LESTR/Fusin and Blocks HIV-1 Entry. *Nature* **1996**, *382*, 829-833; (b) Oberlin, E.; Amara, A.; Bachelerie, F.; Bessia, C.; Virelizier, J. L.; Arenzana-Seisdedos, F.; Schwartz, O.; Heard, J. M.; Clark-Lewis, I.; Legler, D. F.; Loetscher, M.; Baggiolini, M.; Moser, B. The CXC Chemokine SDF-1 is the Ligand for LESTR/Fusin and Prevents Infection by T-Cell-Line-Adapted HIV-1. *Nature* **1996**, *382*, 833-835; (c) Feng, Y.; Broder, C. C.; Kennedy, P. E.; Berger, E. A. HIV-1 Entry Cofactor: Functional cDNA Cloning of a Seven-Transmembrane, G Protein-Coupled Receptor. *Science* **1996**, *272*, 872-877.

8. (a) Tamamura, H.; Fujii, N. The Therapeutic Potential of CXCR4 Antagonists in the Treatment of HIV Infection, Cancer Metastasis and Rheumatoid Arthritis. *Expert Opin Ther*

Targets **2005**, *9*, 1267-1282; (b) Kryczek, I.; Wei, S.; Keller, E.; Liu, R.; Zou, W. Stroma-Derived Factor (SDF-1/CXCL12) and Human Tumor Pathogenesis. *Am J Physiol Cell Physiol* **2007**, *292*, C987-995; (c) Peled, A.; Wald, O.; Burger, J. Development of Novel CXCR4-Based Therapeutics. *Expert Opin Investig Drugs* **2012**, *21*, 341-353.

9. (a) Guo, F.; Wang, Y.; Liu, J.; Mok, S. C.; Xue, F.; Zhang, W. CXCL12/CXCR4: a Symbiotic Bridge Linking Cancer Cells and Their Stromal Neighbors in Oncogenic Communication Networks. *Oncogene* **2016**, *35*, 816-826; (b) Burger, J. A.; Peled, A. CXCR4 Antagonists: Targeting the Microenvironment in Leukemia and Other Cancers. *Leukemia* **2009**, *23*, 43-52.

10. (a) Scotton, C. J.; Wilson, J. L.; Scott, K.; Stamp, G.; Wilbanks, G. D.; Fricker, S.; Bridger, G.; Balkwill, F. R. Multiple Actions of the Chemokine CXCL12 on Epithelial Tumor Cells in Human Ovarian Cancer. *Cancer Res* **2002**, *62*, 5930-5938; (b) Taichman, R. S.; Cooper, C.; Keller, E. T.; Pienta, K. J.; Taichman, N. S.; McCauley, L. K. Use of the Stromal Cell-Derived Factor-1/CXCR4 Pathway in Prostate Cancer Metastasis to Bone. *Cancer Res* **2002**, *62*, 1832-1837; (c) Kim, S. Y.; Lee, C. H.; Midura, B. V.; Yeung, C.; Mendoza, A.; Hong, S. H.; Ren, L.; Wong, D.; Korz, W.; Merzouk, A.; Salari, H.; Zhang, H.; Hwang, S. T.; Khanna, C.; Helman, L. J. Inhibition of the CXCR4/CXCL12 Chemokine Pathway Reduces the Development of Murine Pulmonary Metastases. *Clin Exp Metastasis* **2008**, *25*, 201-211; (d) Koshiba, T.; Hosotani, R.; Miyamoto, Y.; Ida, J.; Tsuji, S.; Nakajima, S.; Kawaguchi, M.; Kobayashi, H.; Doi, R.; Hori, T.; Fujii, N.; Imamura, M. Expression of Stromal Cell-Derived Factor 1 and CXCR4 Ligand Receptor System in Pancreatic Cancer: a Possible Role for Tumor Progression. *Clin Cancer Res* **2000**, *6*, 3530-3535; (e) Hwang, J. H.; Hwang, J. H.; Chung, H. K.; Kim, D. W.; Hwang, E. S.; Suh, J. M.; Kim, H.; You, K. H.; Kwon, O. Y.; Ro, H. K.; Jo, D.

Y.; Shong, M. CXC Chemokine Receptor 4 Expression and Function in Human Anaplastic Thyroid Cancer Cells. *J Clin Endocrinol Metab* **2003**, *88*, 408-416; (f) Muller, A.; Homey, B.; Soto, H.; Ge, N.; Catron, D.; Buchanan, M. E.; McClanahan, T.; Murphy, E.; Yuan, W.; Wagner, S. N.; Barrera, J. L.; Mohar, A.; Verastegui, E.; Zlotnik, A. Involvement of Chemokine Receptors in Breast Cancer Metastasis. *Nature* **2001**, *410*, 50-56; (g) Zlotnik, A., New Insights on the Role of CXCR4 in Cancer Metastasis. *J Pathol* **2008**, *215*, 211-213; (h) Teicher, B. A.; Fricker, S. P., CXCL12 (SDF-1)/CXCR4 Pathway in Cancer. *Clin Cancer Res* **2010**, *16*, 2927-2931; (i) Balkwill, F., The Significance of Cancer Cell Expression of the Chemokine Receptor CXCR4. *Semin Cancer Biol* **2004**, *14*, 171-179.

11. Petit, I.; Jin, D.; Rafii, S. The SDF-1-CXCR4 Signaling Pathway: a Molecular Hub Modulating Neo-Angiogenesis. *Trends Immunol* **2007**, *28*, 299-307.

12. (a) Sultan, M.; Coyle, K. M.; Vidovic, D.; Thomas, M. L.; Gujar, S.; Marcato, P. Hide-and-Seek: the Interplay Between Cancer Stem Cells and the Immune System. *Carcinogenesis* **2017**, *38*, 107-118; (b) Domanska, U. M.; Kruizinga, R. C.; Nagengast, W. B.; Timmer-Bosscha, H.; Huls, G.; de Vries, E. G.; Walenkamp, A. M. A Review on CXCR4/CXCL12 Axis in Oncology: no Place to Hide. *Eur J Cancer* **2013**, *49*, 219-230.

13. (a) Smith, M. C.; Luker, K. E.; Garbow, J. R.; Prior, J. L.; Jackson, E.; Piwnica-Worms, D.; Luker, G. D. CXCR4 Regulates Growth of Both Primary and Metastatic Breast Cancer. *Cancer Res* **2004**, *64*, 8604-8612; (b) Righi, E.; Kashiwagi, S.; Yuan, J.; Santosuosso, M.; Leblanc, P.; Ingraham, R.; Forbes, B.; Edelblute, B.; Collette, B.; Xing, D.; Kowalski, M.; Mingari, M. C.; Vianello, F.; Birrer, M.; Orsulic, S.; Dranoff, G.; Poznansky, M. C. CXCL12/CXCR4 Blockade Induces Multimodal Antitumor Effects that Prolong Survival in an Immunocompetent Mouse Model of Ovarian Cancer. *Cancer Res* **2011**, *71*, 5522-5534; (c) Feig,

C.; Jones, J. O.; Kraman, M.; Wells, R. J.; Deonarine, A.; Chan, D. S.; Connell, C. M.; Roberts, E. W.; Zhao, Q.; Caballero, O. L.; Teichmann, S. A.; Janowitz, T.; Jodrell, D. I.; Tuveson, D. A.; Fearon, D. T. Targeting CXCL12 from FAP-Expressing Carcinoma-Associated Fibroblasts Synergizes with Anti-PD-L1 Immunotherapy in Pancreatic Cancer. *Proc Nat Acad Sci* **2013**, *110*, 20212-20217.

14. Debnath, B.; Xu, S.; Grande, F.; Garofalo, A.; Neamati, N. Small Molecule Inhibitors of CXCR4. *Theranostics* **2013**, *3*, 47-75.

15. (a) De Clercq, E.; Yamamoto, N.; Pauwels, R.; Baba, M.; Schols, D.; Nakashima, H.; Balzarini, J.; Debyser, Z.; Murrer, B. A.; Schwartz, D.; Thorton, D.; Bridger, G.; Fricker, S.; Henson, G.; Abrams, M.; Picker, D. Potent and Selective Inhibition of Human Immunodeficiency Virus (HIV)-1 and HIV-2 Replication by a Class of Bicyclams Interacting with a Viral Uncoating Event. *Proc Nat Acad Sci* **1992**, *89*, 5286-5290; (b) Schols, D.; Struyf, S.; Van Damme, J.; Este, J. A.; Henson, G.; De Clercq, E. Inhibition of T-tropic HIV Strains by Selective Antagonization of the Chemokine Receptor CXCR4. *J Exp Medicine* **1997**, *186*, 1383-1388; (c) Donzella, G. A.; Schols, D.; Lin, S. W.; Este, J. A.; Nagashima, K. A.; Maddon, P. J.; Allaway, G. P.; Sakmar, T. P.; Henson, G.; De Clercq, E.; Moore, J. P. AMD3100, a Small Molecule Inhibitor of HIV-1 Entry via the CXCR4 Co-Receptor. *Nature Medicine* **1998**, *4*, 72-77.

16. (a) De Clercq, E. The Bicyclam AMD3100 Story. *Nature Rev Drug Disc* **2003**, *2*, 581-587; (b) De Clercq, E. The AMD3100 Story: the Path to the Discovery of a Stem Cell Mobilizer (Mozobil). *Biochem Pharm* **2009**, *77*, 1655-1664.

17. (a) Byrne, S. N.; Sarchio, S. N. AMD3100 Protects from UV-Induced Skin Cancer. *Oncoimmunology* **2014**, *3*, e27562; (b) Chen, Y.; Ramjiawan, R. R.; Reiberger, T.; Ng, M. R.;

Hato, T.; Huang, Y.; Ochiai, H.; Kitahara, S.; Unan, E. C.; Reddy, T. P.; Fan, C.; Huang, P.; Bardeesy, N.; Zhu, A. X.; Jain, R. K.; Duda, D. G. CXCR4 Inhibition in Tumor Microenvironment Facilitates Anti-Programmed Death Receptor-1 Immunotherapy in Sorafenib-Treated Hepatocellular Carcinoma in Mice. *Hepatology* **2015**, *61*, 1591-1602; (c) Durr, C.; Pfeifer, D.; Claus, R.; Schmitt-Graeff, A.; Gerlach, U. V.; Graeser, R.; Kruger, S.; Gerbitz, A.; Negrin, R. S.; Finke, J.; Zeiser, R. CXCL12 Mediates Immunosuppression in the Lymphoma Microenvironment After Allogeneic Transplantation of Hematopoietic Cells. *Cancer Res* **2010**, *70*, 10170-10181; (d) Kajiyama, H.; Shibata, K.; Terauchi, M.; Ino, K.; Nawa, A.; Kikkawa, F. Involvement of SDF-1alpha/CXCR4 Axis in the Enhanced Peritoneal Metastasis of Epithelial Ovarian Carcinoma. *Int J Cancer* **2008**, *122*, 91-99; (e) Kawaguchi, A.; Orba, Y.; Kimura, T.; Iha, H.; Ogata, M.; Tsuji, T.; Ainai, A.; Sata, T.; Okamoto, T.; Hall, W. W.; Sawa, H.; Hasegawa, H. Inhibition of the SDF-1alpha-CXCR4 Axis by the CXCR4 Antagonist AMD3100 Suppresses the Migration of Cultured Cells from ATL Patients and Murine Lymphoblastoid Cells from HTLV-I Tax Transgenic Mice. *Blood* **2009**, *114*, 2961-2968; (f) Limon-Flores, A. Y.; Chacon-Salinas, R.; Ramos, G.; Ullrich, S. E. Mast Cells Mediate the Immune Suppression Induced by Dermal Exposure to JP-8 Jet Fuel. *Toxicol Sci* **2009**, *112*, 144-152; (g) Ray, P.; Lewin, S. A.; Mihalko, L. A.; Schmidt, B. T.; Luker, K. E.; Luker, G. D. Noninvasive Imaging Reveals Inhibition of Ovarian Cancer by Targeting CXCL12-CXCR4. *Neoplasia* **2011**, *13*, 1152-1161; (h) Sarchio, S. N.; Scolyer, R. A.; Beaugie, C.; McDonald, D.; Marsh-Wakefield, F.; Halliday, G. M.; Byrne, S. N. Pharmacologically Antagonizing the CXCR4-CXCL12 Chemokine Pathway with AMD3100 Inhibits Sunlight-Induced Skin Cancer. *J Invest Dermatol* **2014**, *134*, 1091-1100; (i) Zhao, E.; Wang, L.; Dai, J.; Kryczek, I.; Wei, S.; Vatan, L.; Altuwaijri, S.; Sparwasser, T.; Wang, G.; Keller, E. T.; Zou, W. Regulatory T Cells in the Bone

Marrow Microenvironment in Patients with Prostate Cancer. *Oncoimmunology* **2012**, *1*, 152-161.

18. Skerlj, R. T.; Bridger, G. J.; Kaller, A.; McEachern, E. J.; Crawford, J. B.; Zhou, Y.; Atsma, B.; Langille, J.; Nan, S.; Veale, D.; Wilson, T.; Harwig, C.; Hatse, S.; Princen, K.; De Clercq, E.; Schols, D. Discovery of Novel Small Molecule Orally Bioavailable C-X-C Chemokine Receptor 4 Antagonists that are Potent Inhibitors of T-Tropic (X4) HIV-1 Replication. *J Med Chem* **2010**, *53*, 3376-3388.

19. (a) Catalano, J. G.; Gudmundsson, K. S.; Svolto, A.; Boggs, S. D.; Miller, J. F.; Spaltenstein, A.; Thomson, M.; Wheelan, P.; Minick, D. J.; Phelps, D. P.; Jenkinson, S. Synthesis of a Novel Tricyclic 1,2,3,4,4a,5,6,10b-Octahydro-1,10-Phenanthroline Ring System and CXCR4 Antagonists with Potent Activity Against HIV-1. *Bioorg Med Chem Lett* **2010**, *20*, 2186-2190; (b) Gudmundsson, K. S.; Boggs, S. D.; Catalano, J. G.; Svolto, A.; Spaltenstein, A.; Thomson, M.; Wheelan, P.; Jenkinson, S. Imidazopyridine-5,6,7,8-Tetrahydro-8-Quinolinamine Derivatives with Potent Activity Against HIV-1. *Bioorg Med Chem Lett* **2009**, *19*, 6399-6403; (c) Gudmundsson, K. S.; Sebahar, P. R.; Richardson, L. D.; Miller, J. F.; Turner, E. M.; Catalano, J. G.; Spaltenstein, A.; Lawrence, W.; Thomson, M.; Jenkinson, S. Amine Substituted N-(1H-Benzimidazol-2ylmethyl)-5,6,7,8-Tetrahydro-8-Quinolinamines as CXCR4 Antagonists with Potent Activity Against HIV-1. *Bioorg Med Chem Lett* **2009**, *19*, 5048-5052; (d) Miller, J. F.; Gudmundsson, K. S.; D'Aurora Richardson, L.; Jenkinson, S.; Spaltenstein, A.; Thomson, M.; Wheelan, P. Synthesis and SAR of Novel Isoquinoline CXCR4 Antagonists with Potent Anti-HIV activity. *Bioorg Med Chem Lett* **2010**, *20*, 3026-3030; (e) Jenkinson, S.; Thomson, M.; McCoy, D.; Edelstein, M.; Danehower, S.; Lawrence, W.; Wheelan, P.; Spaltenstein, A.; Gudmundsson, K. Blockade of X4-Tropic HIV-1 Cellular Entry by GSK812397, a Potent

Noncompetitive CXCR4 Receptor Antagonist. *Antimicrob Agents Chemother* **2010**, *54*, 817-824; (f) Miller, J. F.; Turner, E. M.; Gudmundsson, K. S.; Jenkinson, S.; Spaltenstein, A.; Thomson, M.; Wheelan, P., Novel N-Substituted Benzimidazole CXCR4 Antagonists as Potential Anti-HIV Agents. *Bioorg Med Chem Lett* **2010**, *20*, 2125-2128.

20. Thoma, G.; Streiff, M. B.; Kovarik, J.; Glickman, F.; Wagner, T.; Beerli, C.; Zerwes, H. G. Orally Bioavailable Isothioureas Block Function of the Chemokine Receptor CXCR4 in Vitro and in Vivo. *J Med Chem* **2008**, *51*, 7915-7920.

21. (a) Zhan, W.; Liang, Z.; Zhu, A.; Kurtkaya, S.; Shim, H.; Snyder, J. P.; Liotta, D. C. Discovery of Small Molecule CXCR4 Antagonists. *J Med Chem* **2007**, *50*, 5655-5664; (b) Zhao, H.; Prosser, A. R.; Liotta, D. C.; Wilson, L. J. Discovery of Novel N-Aryl Piperazine CXCR4 Antagonists. *Bioorg Med Chem Lett* **2015**, *25*, 4950-4955; (c) Truax, V. M.; Zhao, H.; Katzman, B. M.; Prosser, A. R.; Alcaraz, A. A.; Saindane, M. T.; Howard, R. B.; Culver, D.; Arrendale, R. F.; Gruddanti, P. R.; Evers, T. J.; Natchus, M. G.; Snyder, J. P.; Liotta, D. C.; Wilson, L. J. Discovery of Tetrahydroisoquinoline-Based CXCR4 Antagonists. *ACS Med Chem Lett* **2013**, *4*, 1025-1030.

22. Wilson, R. J.; Jecs, E.; Miller, E. J.; Nguyen, H. H.; Tahirovic, Y. A.; Truax, V. M.; Kim, M. B.; Kuo, K. M.; Wang, T.; Sum, C. S.; Cvijic, M. E.; Paiva, A. A.; Schroeder, G. M.; Wilson, L. J.; Liotta, D. C. Synthesis and SAR of 1,2,3,4-Tetrahydroisoquinoline-Based CXCR4 Antagonists. *ACS Med Chem Lett* **2018**, *9*, 17-22.

23. Veber, D. F.; Johnson, S. R.; Cheng, H. Y.; Smith, B. R.; Ward, K. W.; Kopple, K. D. Molecular Properties that Influence the Oral Bioavailability of Drug Candidates. *J Med Chem* **2002**, *45*, 2615-2623.

24. (a) Stucchi, M.; Gmeiner, P.; Huebner, H.; Rainoldi, G.; Sacchetti, A.; Silvani, A.; Lesma, G. Multicomponent Synthesis and Biological Evaluation of a Piperazine-Based Dopamine Receptor Ligand Library. *ACS Med Chem Lett* **2015**, *6*, 882-887; (b) Peng, H.; Kumaravel, G.; Yao, G.; Sha, L.; Wang, J.; Van Vlijmen, H.; Bohnert, T.; Huang, C.; Vu, C. B.; Ensinger, C. L.; Chang, H.; Engber, T. M.; Whalley, E. T.; Petter, R. C. Novel Bicyclic Piperazine Derivatives of Triazolotriazine and Triazolopyrimidines as Highly Potent and Selective Adenosine A2A Receptor Antagonists. *J Med Chem* **2004**, *47*, 6218-6229; (c) Venable, J. D.; Cai, H.; Chai, W.; Dvorak, C. A.; Grice, C. A.; Jablonowski, J. A.; Shah, C. R.; Kwok, A. K.; Ly, K. S.; Pio, B.; Wei, J.; Desai, P. J.; Jiang, W.; Nguyen, S.; Ling, P.; Wilson, S. J.; Dunford, P. J.; Thurmond, R. L.; Lovenberg, T. W.; Karlsson, L.; Carruthers, N. I.; Edwards, J. P. Preparation and Biological Evaluation of Indole, Benzimidazole, and Thienopyrrole Piperazine Carboxamides: Potent Human Histamine H(4) Antagonists. *J Med Chem* **2005**, *48*, 8289-8298; (d) Di Fabio, R.; Griffante, C.; Alvaro, G.; Pentassuglia, G.; Pizzi, D. A.; Donati, D.; Rossi, T.; Guercio, G.; Mattioli, M.; Cimarosti, Z.; Marchioro, C.; Provera, S.; Zonzini, L.; Montanari, D.; Melotto, S.; Gerrard, P. A.; Trist, D. G.; Ratti, E.; Corsi, M. Discovery Process and Pharmacological Characterization of 2-(S)-(4-Fluoro-2-methylphenyl)piperazine-1-carboxylic acid [1-(R)-(3,5-Bis-trifluoromethylphenyl)ethyl]methylamide (Vestipitant) as a Potent, Selective, and Orally Active NK1 Receptor Antagonist. *J Med Chem* **2009**, *52*, 3238-3247; (e) Chen, C.; Pontillo, J.; Fleck, B. A.; Gao, Y.; Wen, J.; Tran, J. A.; Tucci, F. C.; Marinkovic, D.; Foster, A. C.; Saunders, J. 4-{(2R)-[3-Aminopropionylamido]-3-(2,4-dichlorophenyl)propionyl}-1-{2-[(2-thienyl)ethylaminomethyl]phenyl}piperazine as a Potent and Selective Melanocortin-4 Receptor Antagonist-Design, Synthesis, and Characterization. *J Med Chem* **2004**, *47*, 6821-6830; (f) Nirogi, R.; Shinde, A.; Kambhampati, R. S.; Mohammed,

A. R.; Saraf, S. K.; Badange, R. K.; Bandyala, T. R.; Bhatta, V.; Bojja, K.; Reballi, V.; Subramanian, R.; Benade, V.; Palacharla, R. C.; Bhyrapuneni, G.; Jayarajan, P.; Goyal, V.; Jasti, V. Discovery and Development of 1-[(2-Bromophenyl)sulfonyl]-5-methoxy-3-[(4-methyl-1-piperazinyl)methyl]-1H-indole Dimesylate Monohydrate (SUVN-502): A Novel, Potent, Selective and Orally Active Serotonin 6 (5-HT6) Receptor Antagonist for Potential Treatment of Alzheimer's Disease. *J Med Chem* **2017**, *60*, 1843-1859; (g) Thomas, J. B.; Atkinson, R. N.; Rothman, R. B.; Fix, S. E.; Mascarella, S. W.; Vinson, N. A.; Xu, H.; Dersch, C. M.; Lu, Y.; Cantrell, B. E.; Zimmerman, D. M.; Carroll, F. I. Identification of the First Trans-(3R,4R)-dimethyl-4-(3-hydroxyphenyl)piperidine Derivative to Possess Highly Potent and Selective Opioid Kappa Receptor Antagonist Activity. *J Med Chem* **2001**, *44*, 2687-2690.

25. (a) Tagat, J. R.; McCombie, S. W.; Nazareno, D.; Labroli, M. A.; Xiao, Y.; Steensma, R. W.; Strizki, J. M.; Baroudy, B. M.; Cox, K.; Lachowicz, J.; Varty, G.; Watkins, R. Piperazine-Based CCR5 Antagonists as HIV-1 Inhibitors. IV. Discovery of 1-[(4,6-Dimethyl-5-pyrimidinyl)carbonyl]- 4-[4-[2-methoxy-1(R)-4-(trifluoromethyl)phenyl]ethyl-3(S)-methyl-1-piperazinyl]- 4-methylpiperidine (Sch-417690/Sch-D), a Potent, Highly Selective, and Orally Bioavailable CCR5 Antagonist. *J Med Chem* **2004**, *47*, 2405-2408; (b) Tagat, J. R.; Steensma, R. W.; McCombie, S. W.; Nazareno, D. V.; Lin, S. I.; Neustadt, B. R.; Cox, K.; Xu, S.; Wojcik, L.; Murray, M. G.; Vantuno, N.; Baroudy, B. M.; Strizki, J. M. Piperazine-Based CCR5 Antagonists as HIV-1 Inhibitors. II. Discovery of 1-[(2,4-Dimethyl-3-pyridinyl)carbonyl]-4-methyl-4-[3(S)-methyl-4-[1(S)-[4-(trifluoromethyl)phenyl]ethyl]-1-piperazinyl]- piperidine N1-oxide (Sch-350634), an Orally Bioavailable, Potent CCR5 Antagonist. *J Med Chem* **2001**, *44*, 3343-3346; (c) Habashita, H.; Kokubo, M.; Hamano, S.; Hamanaka, N.; Toda, M.; Shibayama, S.; Tada, H.; Sagawa, K.; Fukushima, D.; Maeda, K.; Mitsuya, H. Design, Synthesis, and

Biological Evaluation of the Combinatorial Library with a New Spirodiketopiperazine Scaffold. Discovery of Novel Potent and Selective Low-Molecular-Weight CCR5 Antagonists. *J Med Chem* **2006**, *49*, 4140-4152.

26. Andrews, S. P.; Cox, R. J. Small Molecule CXCR3 Antagonists. *J Med Chem* **2016**, *59*, 2894-2917.

27. Digby, G. J.; Shirey, J. K.; Conn, P. J. Allosteric Activators of Muscarinic Receptors as Novel Approaches for Treatment of CNS Disorders. *Molecular bioSystems* **2010**, *6*, 1345-1354.

28. Beadle, C. D.; Coates, D.A.; Hao, J.; Krushinski, J.H.Jr.; Reinhard, M.R.; Schaus, J.M.; Wolfangel, C.D. Preparation of [2-(2-Phenylacetyl)-1,2,3,4-Tetrahydroisoquinolin-3-yl]methanol Derivatives as Positive Allosteric Modulators (PAMs) of Dopamine 1 Receptor (D1). PCT Int. Appl. 2014193781 (2014).

29. Reverse phase chiral HPLC (254 and 210 nm): gradient 55-60 ACN for 30 min at 0.5 mL/min on Chiral OD-RH column.

30. Normal phase chiral HPLC (254 and 210 nm): 10% IPA/hexanes isocratic for 40 min at 1.0 mL/min, t1 = 8.894, t2 = 10.346.

31. Yang, Z.; Zadjura, L. M.; Marino, A. M.; D'Arienzo, C. J.; Malinowski, J.; Gesenberg, C.; Lin, P. F.; Colonno, R. J.; Wang, T.; Kadow, J. F.; Meanwell, N. A.; Hansel, S. B. Utilization of In Vitro Caco-2 Permeability and Liver Microsomal Half-Life Screens in Discovering BMS-488043, a Novel HIV-1 Attachment Inhibitor with Improved Pharmacokinetic Properties. *J Pharma Sci* **2010**, *99*, 2135-2152.

32. Zhu, C.; Jiang, L.; Chen, T. M.; Hwang, K. K. A Comparative Study of Artificial Membrane Permeability Assay for High Throughput Profiling of Drug Absorption Potential. *Eur J Med Chem* **2002**, *37*, 399-407.

33. Skerlj, R.; Bridger, G.; McEachern, E.; Harwig, C.; Smith, C.; Kaller, A.; Veale, D.; Yee, H.; Skupinska, K.; Wauthy, R.; Wang, L.; Baird, I.; Zhu, Y.; Burrage, K.; Yang, W.; Sartori, M.; Huskens, D.; De Clercq, E.; Schols, D. Design of Novel CXCR4 Antagonists that are Potent Inhibitors of T-Tropic (X4) HIV-1 Replication. *Bioorg Med Chem Lett* **2011**, *21*, 1414-1418.

34. Calculated by ChemDraw 15.

35. Leeson, P. D.; Springthorpe, B. The Influence of Drug-Like Concepts on Decision-Making in Medicinal Chemistry. *Nature Rev Drug Disc* **2007**, *6*, 881-890.

36. Hitchcock, S. A. Structural Modifications that Alter the P-Glycoprotein Efflux Properties of Compounds. *J Med Chem* **2012**, *55*, 4877-4895.

37. (a) Wuitschik, G.; Carreira, E. M.; Wagner, B.; Fischer, H.; Parrilla, I.; Schuler, F.; Rogers-Evans, M.; Muller, K. Oxetanes in Drug Discovery: Structural and Synthetic Insights. *J Med Chem* **2010**, *53*, 3227-3246; (b) Burkhard, J. A.; Wuitschik, G.; Rogers-Evans, M.; Muller, K.; Carreira, E. M. Oxetanes as Versatile Elements in Drug Discovery and Synthesis. *Ang Chem Int Ed Eng* **2010**, *49*, 9052-9067.

38. Kieltyka, K.; Zhang, J.; Li, S.; Vath, M.; Baglieri, C.; Ferraro, C.; Zvyaga, T. A.; Drexler, D. M.; Weller, H. N.; Shou, W. Z. A High-Throughput Bioanalytical Platform Using Automated Infusion for Tandem Mass Spectrometric Method Optimization and Its Application in a Metabolic Stability Screen. *Rapid Commun Mass Spectrom* **2009**, *23*, 1579-1591.

39. Boggs, S.; Elitzin, V. I.; Gudmundsson, K.; Martin, M. T.; Sharp, M. J. Kilogram-Scale Synthesis of the CXCR4 Antagonist GSK812397. *Org Proc Res Dev* **2009**, *13*, 781-785.

40. McEachern, E. J.; Bridger, G.J.; Skupinska, K.A.; Skerlj, R.T. Synthesis of Enantiomerically Pure Amino-Substituted Fused Bicyclic Rings. PCT Int. Appl., 2003022785 (2003).

41. Wu, B.; Chien, E. Y.; Mol, C. D.; Fenalti, G.; Liu, W.; Katritch, V.; Abagyan, R.; Brooun, A.; Wells, P.; Bi, F. C.; Hamel, D. J.; Kuhn, P.; Handel, T. M.; Cherezov, V.; Stevens, R. C. Structures of the CXCR4 Chemokine GPCR with Small-Molecule and Cyclic Peptide Antagonists. *Science* **2010**, *330*, 1066-1071.

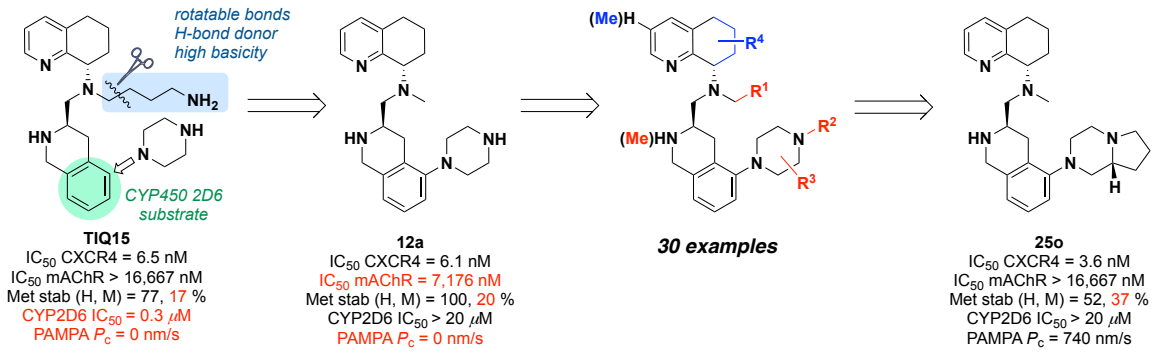
rotatable bonds
H-bond donor
high basicity
CYP450 2D6
substrate
TIQ15
IC50 CXCR4 = 6.5 nM
IC50 mAChR > 16,667 nM
Met stab (H, M) = 77, 17 %
CYP2D6 IC50 = 0.3 μM
PAMPA Pc = 0 nm/s
12a
IC50 CXCR4 = 6.1 nM
IC50 mAChR = 7,176 nM
Met stab (H, M) = 100, 20 %
CYP2D6 IC50 > 20 μM
PAMPA Pc = 0 nm/s
30 examples
25o
IC50 CXCR4 = 3.6 nM
IC50 mAChR > 16,667 nM
Met stab (H, M) = 52, 37 %
CYP2D6 IC50 > 20 μM
PAMPA Pc = 740 nm/s